Author Contributions:

Conceptualization: J. L. Hand, A. J. Prenni, B. A. Schichtel
Formal analysis: J. L. Hand
Methodology: J. L. Hand, A. J. Prenni, B. A. Schichtel
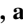**Visualization:** J. L. Hand, A. J. Prenni, S. M. Raffuse
Writing – original draft: J. L. Hand
Writing – review & editing: J. L. Hand, A. J. Prenni, S. M. Raffuse, N. P. Hyslop, W. C. Malm, B. A. Schichtel

Spatial and Seasonal Variability of Remote and Urban Speciated Fine Particulate Matter in the United States

J. L. Hand[1] , A. J. Prenni[2] , S. M. Raffuse[3] , N. P. Hyslop[3] , W. C. Malm[1] , and B. A. Schichtel[2]

[1]Cooperative Institute for Research in the Atmosphere, Colorado State University, Fort Collins, CO, USA, [2]National Park Service, Air Resources Division, Lakewood, CO, USA, [3]Air Quality Research Center, University of California Davis, Davis, CA, USA

Abstract The spatial and seasonal variability in the composition of major $PM_{2.5}$ (particles with aerodynamic diameters less than 2.5 μm) aerosol species in the United States were characterized using data from ground-based aerosol monitoring networks. The IMPROVE (Interagency Monitoring of Protected Visual Environments) network and the Chemical Speciation Network (CSN) operate in mostly rural/remote or urban/suburban sites, respectively. The networks have similar sampling schedules and analysis methods. Regional, monthly, and annual mean concentrations from 2019 to 2022 were calculated for ammonium sulfate (AS), ammonium nitrate (AN), particulate organic matter (POM), elemental carbon (EC), fine dust (FD), and sea salt (SS), as well as their relative contributions to reconstructed $PM_{2.5}$ mass (RCFM). Organic aerosols were the largest contributor to RCFM across the United States (>40% annually, up to 80% monthly), with significant impacts from biomass smoke on POM and EC concentrations, contributions, and seasonality. AS concentrations and contributions were similar in urban and rural regions and contributed <20% annually to RCFM, considerably less than two decades ago. In general, urban concentrations were greater for AN, POM, and EC, suggesting additional urban sources. Some species, such as POM, FD, and AN, exhibited strong seasonal variability due to episodic source impacts or seasonal formation conditions. Evaluating the urban and rural monthly variability of major aerosol species is necessary for understanding the impacts of emission sources, regional transport, and atmospheric processes governing aerosol concentrations in the atmosphere.

Plain Language Summary Particulate matter (PM) in the atmosphere is made of up of many types of aerosols that can differ in urban and rural settings depending on sources, atmospheric processes, and transport. Combining data from large urban and rural ground-based aerosol monitoring programs in the United States revealed differences in the seasonal and spatial variability of urban and rural aerosols. For example, nitrate, organic carbon, and elemental carbon concentrations were higher in urban areas due to additional urban sources, while sulfate levels in urban and rural regions were similar. Some species were highly seasonal due to their formation conditions occurring in specific seasons or influence from episodic emissions like wildfire smoke. Smoke strongly influenced aerosol composition across the western United States due to high fire years during the study period. Organic carbon is now the major contributor to both urban and rural PM in the United States, in part due to the successful regulatory activity that removed sulfate mass, and the increased contributions from wildfire smoke. Examining the seasonal and spatial variability in aerosol composition is necessary to understand the role of natural and anthropogenic source impacts on PM and to develop strategies to reduce PM in the atmosphere.

1. Introduction

Characterizing the spatial and seasonal variability in the composition of major aerosol species is essential for quantifying their impacts on the environment, human health, visibility, and climate. Estimating the contribution of major aerosol species to $PM_{2.5}$ (particles with aerodynamic diameters less than 2.5 μm) mass is necessary for identifying sources, regional transport, and deposition of aerosols. Previous studies have demonstrated that absolute and relative concentrations of major aerosol species vary significantly depending on region and season (e.g., Blanchard et al., 2013; Cheng et al., 2024; Hand, Schichtel, & Pitchford et al., 2012; Hand et al., 2020, 2024; Malm et al., 1994, 2004, 2011; Malm & Hand, 2007; Simon et al., 2011) and have changed dramatically over time as both regulated and unregulated emissions have changed (e.g., Attwood et al., 2014; Beachley et al., 2016; Benish et al., 2022; Cheng et al., 2024; Du et al., 2014; Ellis et al., 2013; Feng et al., 2020; Hand, Schichtel, & Malm

et al., 2012; Hand et al., 2016, 2017, 2020, 2024; Lawal et al., 2018; Lehmann & Gay, 2011; Malm et al., 2002, 2017; Nopmongcol et al., 2019; Prenni et al., 2019; Sickles & Shadwick, 2015; Zhang et al., 2018). Emission changes can alter the seasonality of major aerosol species (Chan et al., 2018; Shah et al., 2018) which influences their environmental and climate impacts.

Ground-based aerosol monitoring networks provide data that are critical for understanding the seasonal and spatial variability of major aerosol species in the United States. The IMPROVE (Interagency Monitoring of Protected Visual Environments) network began operating in 1988 to track trends in aerosol composition and haze in remote and rural areas (Malm et al., 1994). Since 2000 the IMPROVE network also provides monitoring to support the Environmental Protection Agency's (EPA) Regional Haze Rule (RHR) (EPA, 2003, 2018). EPA's Chemical Speciation Network (CSN) began operating in 2000 in urban and suburban sites to track progress of emission reduction strategies and support health effect and exposure studies (Solomon et al., 2014). The IMPROVE network and the CSN have similar sampling schedules and sampling and analysis methods (Gorham et al., 2021; Hand et al., 2023; Solomon et al., 2014). Data from both networks have been aggregated to extend monitoring coverage across the United States, to understand urban impacts on rural areas (Frank, 2006; Hand, Schichtel, & Pitchford et al., 2012; Hand et al., 2014; Malm et al., 2011), and to understand sampling biases and analytical differences (Gorham et al., 2021; Malm et al., 2011; Solomon et al., 2014; Spada & Hyslop, 2018; Zhang et al., 2022).

Particulate matter (PM) is derived from both primary and secondary sources, as well as natural and anthropogenic emissions. The major species contributing to PM include sulfate, nitrate, carbonaceous aerosols, mineral dust, and sea salt. Contributions from these species to PM are assessed by approximating their molecular forms in the atmosphere. These approximations are based on detailed scientific measurements and analyses (e.g., Chow, Lowenthal, et al., 2015). In addition, comparisons between reconstructed fine mass (RCFM = sum of individual species mass) to gravimetric $PM_{2.5}$ mass can lend insight into appropriate assumptions of molecular forms. For example, Hand et al. (2019) identified biases in the $PM_{2.5}$ reconstruction mass algorithm as applied to data from the IMPROVE network that were associated with organic mass and mineral dust, as well as assumptions regarding the molecular form of sulfate aerosols.

The majority of sulfate in the atmosphere is produced through chemical transformations of gaseous sulfur dioxide (SO_2). SO_2 is emitted through industrial activities such as coal and diesel fuel combustion. Regions with high SO_2 emissions and humidity provide conditions that are conducive for sulfate formation, leading to regional-scale impacts that influence rural and urban areas (e.g., Hand, Schichtel, & Pitchford et al., 2012; Hand, Schichtel, & Malm et al., 2012; Hand et al., 2014). The degree of acidity of sulfate (from acidic sulfuric acid to fully neutralized ammonium sulfate, AS) depends on the availability of ammonia to neutralize the sulfuric acid formed from SO_2. Sulfate acidity can vary spatially and temporally (e.g., Lawal et al., 2018) and studies have suggested that sulfate is more acidic in the eastern United States (Chen et al., 2019; Hidy et al., 2014; Kim et al., 2015; Lawal et al., 2018; Lowenthal et al., 2015; Silvern et al., 2017; Weber et al., 2016).

Ammonium nitrate (AN) forms from the reversible reaction of gas-phase ammonia and nitric acid. Sources of oxidized nitrogen include high temperature processes such as combustion of fossil fuels in coal-fired powered plants, biomass burning, on-road, and off-road mobile sources, and biogenic sources such as soil emissions (Vitousek et al., 1997). Sources of ammonia include agricultural activities, such as animal husbandry, fertilizer application, as well as mobile sources and natural emissions. Lower temperatures and higher relative humidity favor particulate AN formation. Nitrate is often assumed to be fine mode AN, and this is probably a reasonable assumption in regions with high ammonia and nitric acid concentrations and low sulfate concentrations (Lee et al., 2008). Urban AN concentrations tend to be higher than concentrations in rural areas (Hand, Schichtel, & Pitchford et al., 2012; Hand et al., 2014) due to higher nitrogen oxides (NO_x) emissions. Elevated AN concentrations in the rural areas in the central United States have been associated with agricultural activity that result in high fine mode nitrate and ammonium concentrations (Heald et al., 2012; Hu et al., 2020; Pitchford et al., 2009; Warner et al., 2017). However, Lee et al. (2008) showed that in many locations, nitrate is associated with the coarse mode from reactions of gas-phase nitric acid with sea salt or calcium carbonate. Allen et al. (2015) observed coarse nitrate during the 2013 Southern Oxidant and Aerosol Study in the Southeast, and Malm et al. (2007) reported regions and seasons with high nitrate concentrations in the coarse mode at a subset of IMPROVE sites.

Carbonaceous aerosols include both organic carbon (OC) and elemental carbon (EC). OC is formed from both primary emissions and secondary formation. Primary emissions include particles emitted directly from combustion of fossil fuels or biomass. Secondary organic aerosol formation results from the oxidation of gas-phase precursors from both anthropogenic and biogenic sources (Blanchard et al., 2016; Schichtel et al., 2017). OC concentrations in urban areas tend to have different seasonality than in rural areas, with higher urban winter concentrations and higher rural summer concentrations due to different sources (Blanchard et al., 2016; Hand, Schichtel, & Pitchford et al., 2012; Hand, Schichtel, & Malm et al., 2012; Hand et al., 2013, 2014). Particulate organic matter (POM) is calculated from OC measurements using an average organic mass (OM) to OC ratio (OM/OC) that accounts for additional elements associated with measured carbon, such as nitrogen, oxygen, and hydrogen. It is common for a significant portion of organic aerosol mass to remain unidentified (Heald & Kroll, 2020; Jimenez et al., 2009; Turpin et al., 2000); therefore, the approach for accounting for other elements in POM mass has been to apply an average OM/OC ratio. Typical OM/OC values range from 1.2 to 2.6, with seasonal and regional variability. For example, values in warm months tend to be higher than cold months, and values in rural areas tend to be higher than in urban areas (e.g., Aiken et al., 2008; Bae et al., 2006; El-Zanan et al., 2005, 2009; Hallar et al., 2013; Kim & Hopke, 2004; Lowenthal et al., 2009; Malm et al., 2011; Philip et al., 2014; Polidori et al., 2008; Ruthenburg et al., 2014; Simon et al., 2011). Elemental carbon (EC) is emitted directly from incomplete combustion of fossil fuels or biomass (e.g., Bond et al., 2013) and is often also referred to as light absorbing carbon or black carbon depending on the measurement method (Petzold et al., 2013). EC concentrations tend to be higher in urban areas due to additional urban sources (Blanchard et al., 2016; Hand, Schichtel, & Pitchford et al., 2012; Hand et al., 2013, 2014) and have been identified as harmful to human health (e.g., Shi et al., 2022; Wei et al., 2023).

Sources of mineral dust in the atmosphere include entrainment from drylands, paved and unpaved roads, agricultural activity, construction, and fire. Dust in the United States is influenced by local, regional, and long-range transport. Contributions of Asian dust to U.S. fine ($PM_{2.5}$) dust concentrations can be significant episodically, affecting aerosol concentrations and elemental composition across the United States, typically in the spring (e.g., Creamean et al., 2014; Hand et al., 2017; Husar et al., 2001; Kim et al., 2021; Prospero et al., 2002). Transport of North African dust to the United States occurs regularly in summer, affecting aerosol concentrations in the Virgin Islands, the eastern and southeastern United States (Aldhaif et al., 2020; Bozlaker et al., 2019; Hand et al., 2017; Perry et al., 1997; Prospero et al., 2021), and even as far as west Texas (Hand et al., 2002). Dust concentrations in desert regions of the Southwest are high due to the impacts of local and regional sources as well as transport from the Chihuahuan desert in Mexico, especially in winter and spring (Hand et al., 2016, 2017; Rivera et al., 2009; Tong et al., 2012). Dust is also emitted by agricultural activity (Ginoux et al., 2012; Hand et al., 2017; Lambert et al., 2020; Pi et al., 2018; Pu & Ginoux, 2018).

Sea salt aerosols form through bubble-bursting at the sea surface. Sea salt (SS) can be a significant contributor to PM at many coastal locations (e.g., Hand, Schichtel, & Pitchford et al., 2012; Lowenthal & Kumar, 2006; Murphy et al., 2019). It is estimated that sea salt is mainly composed of sodium and chloride (White, 2008); however, gas phase reactions of fine particle sodium chloride with nitric and sulfuric acid in the atmosphere can result in chlorine displacement to the gas-phase (Newberg et al., 2005), which can result in an underestimate of SS if chloride is used to estimate it.

The absolute concentrations of the above species and their contributions to $PM_{2.5}$ mass vary spatially and seasonally depending on sources, atmospheric processes, and transport. Evaluating aerosol composition at urban (CSN) and rural (IMPROVE) sites can help elucidate some of these sources and processes. Malm et al. (2004) evaluated data from rural IMPROVE regions in 2001, followed by a study by Hand, Schichtel, & Pitchford et al. (2012) that compared aerosol composition in 2005–2008 in urban CSN and rural IMPROVE regions across the United States to highlight similarities and differences in absolute concentration, relative contribution of individual species to $PM_{2.5}$ mass, and their seasonality. Results from that work demonstrated the importance of sulfate in reconstructed fine mass at both urban and rural sites, with maximum contributions in the eastern United States around 66%. POM contributions were around 20%–30% in the East and over 50% in the West. Since then, trend analyses have demonstrated the effectiveness of precursor emission reductions at removing sulfate, and other species such as nitrate and OC, from the atmosphere (e.g., Hand et al., 2024), thereby shifting the composition of $PM_{2.5}$ mass (Cheng et al., 2024; Hand et al., 2024). Increases in emissions from natural sources, such as wildfire smoke, have contributed to this shift. Here, we update these previous analyses (Hand, Schichtel, & Pitchford et al., 2012; Malm et al., 2004) using similar methodology to identify the current large-scale seasonal

and spatial variability of urban and rural speciated mass concentrations in the context of changing source emissions. Monthly and regional mean results are organized by species for major areas of the country. Comparisons of aerosol composition and speciated contributions to the $PM_{2.5}$ mass budget highlight the importance of local, regional, and long-range/international sources and helps elucidate the atmospheric processes and transport that lead to aerosol seasonal and spatial patterns observed across the United States. Ultimately, identifying the major contributions of aerosol species to $PM_{2.5}$ mass can assist in designing mitigation strategies to reduce $PM_{2.5}$ in the United States and highlight the importance of natural sources to the $PM_{2.5}$ budget, especially as these sources will likely increase in a changing climate.

2. Methodology

2.1. Monitoring Networks

The IMPROVE network has been operating since 1988 (Malm et al., 1994). The network collects 24 hr filters every third day from midnight-to-midnight local standard time at mostly remote and rural sites, and data are reported at ambient conditions. Filters are shipped without controlled temperature conditions. The IMPROVE sampler consists of four independent modules (A, B, C, and D), each collecting filters designed for a specific chemical analysis, and each using a separate inlet. Modules A, B, and C are equipped with $PM_{2.5}$ inlets and module D is equipped with a PM_{10} (particles with aerodynamic diameters less than 10 μm) inlet. $PM_{2.5}$ gravimetric fine mass (also referred to as fine mass, FM), elemental analysis from X-ray fluorescence (XRF), and filter light absorption are determined from Teflon filters collected with module A. $PM_{2.5}$ anions (sulfate, nitrate, and chloride) are analyzed using ion chromatography (IC) on nylon filters collected with module B. $PM_{2.5}$ carbonaceous aerosols (OC and EC) are analyzed using the IMPROVE-A thermal optical analysis (TOA) protocol on quartz filters collected with module C (Chow et al., 2007; Chow, & Wang et al., 2015). All concentrations were reported with blank corrections. Data were used as reported, with no substitutions for values below minimum detection limits. Additional details regarding IMPROVE sampling and artifact corrections are provided by Hand et al. (2023). IMPROVE data were downloaded from the Federal Land Manager Environmental Database (FED; https://views.cira.colostate.edu/fed/, accessed 10 October 2023).

The CSN was deployed in the fall of 2000 (EPA, 2004). The CSN samplers operate on a 24 hr schedule from midnight to midnight every third or every sixth day depending on site, and data are reported at local ambient conditions. Filters are cold shipped to reduce artifacts (Dillner et al., 2009). A detailed description of network operation and sampling details is provided by Solomon et al. (2014). Historically, the CSN utilized several types of samplers, including the Thermo Andersen RAAS, Met One SASS, and the URG MASS. The specific sampler employed at a given site was chosen by the state, local, or tribal agency. Currently, each site operates a Met One SASS or SuperSASS for collection of Teflon (for elemental concentration analysis using XRF) or nylon filters (for cation and anion concentrations using IC). A URG 3000N sampler is used for collection of quartz filters for TOA (Gorham et al., 2021; Malm et al., 2011; Solomon et al., 2014; Spada & Hyslop, 2018). All samplers are equipped with $PM_{2.5}$ inlets. Concentrations are reported with blank corrections (Gorham et al., 2021) and no substitutions were performed for values below minimum detection limits. CSN data were downloaded from the FED database (accessed 10 October 2023).

By the end of 2014 CSN stopped analyzing filters for $PM_{2.5}$ gravimetric mass, instead relying on collocated $PM_{2.5}$ FRM (Federal Reference Method) samplers for $PM_{2.5}$ gravimetric fine mass (FM). In November 2015, contract modifications led to changes in the laboratories responsible for analysis (Young, 2015), including XRF, IC, and TOA, with changes in TOA carbon analysis hardware taking effect in October of 2018 (Gorham et al., 2021; Kaur et al., 2024; Zhang et al., 2022). Several other changes occurred to data processing methods and blank correction applications (Young, 2015). Kaur et al. (2024) showed that these changes in analysis have led to discontinuities in the data and they developed correction factors to evaluate long-term trends. Without adjustments for these disruptions, trends in CSN data should be interpreted with caution. Previous changes in sampling and analytical methods (prior to 2010) are reported and discussed by Malm et al. (2011) and Hand, Schichtel, & Pitchford et al. (2012). Additional details regarding CSN sampling and analysis are reported by Hand et al. (2023).

2.2. Estimates of Aerosol Mass Concentrations

Estimating the mass associated with speciated composition requires assumptions about the molecular form of assumed species. Table 1 presents the algorithms used to reconstruct fine mass for both IMPROVE and the CSN

Table 1

The Form of Molecular Species Assumed to Calculate PM$_{2.5}$ Aerosol Species Concentration

PM$_{2.5}$ aerosol species	Formula	Assumptions
Ammonium Sulfate (AS = $(NH_4)_2SO_4$)	$1.375 \times [SO_4^{2-}]$	Sulfate $[SO_4^{2-}]$ is assumed to be fully neutralized.
Ammonium Nitrate (AN = NH_4NO_3)	$1.29 \times [NO_3^-]$	Nitrate $[NO_3^-]$ is assumed to be ammonium nitrate.
Particulate Organic Matter (POM)	$(OM/OC) \times [OC]$	A monthly varying value OM/OC ratio was used for IMPROVE; seasonal-varying values were used for CSN (see text).
Elemental Carbon (EC)	EC	
IMPROVE Fine Dust (FD)	$2.53 \times [Al] + 2.86 \times [Si] + 1.87 \times [Ca] + 2.78 \times [Fe] + 2.23 \times [Ti]$	Based on the IMPROVE dust formula (Malm et al., 1994) with mass multipliers increased by 15% (see text).
CSN Fine Dust (FD)	$2.20 \times [Al] + 2.49 \times [Si] + 1.63 \times [Ca] + 2.42 \times [Fe] + 1.94 \times [Ti]$	Based on the IMPROVE dust formula (Malm et al., 1994).
Sea Salt (SS)	$1.8 \times [Cl^-]$	Sea salt is 55% chloride ion by weight.

Note. Assumptions were applied to both IMPROVE and CSN data unless otherwise noted.

unless otherwise noted. Sulfate is assumed to be fully neutralized AS and nitrate is assumed to be in the form of AN. Fine dust (FD) was estimated assuming normal oxides of elements typically associated with soil (Malm et al., 1994), but mass multipliers were increased by 15% for IMPROVE data based on an analysis by Hand et al. (2019) that suggested FD was underestimated by the traditional IMPROVE dust algorithm. No similar adjustment was made for CSN FD estimates because a similar analysis does not exist to support the change. Sea salt (SS) was calculated using chloride ion data (White, 2008), recognizing, however that SS may be underestimated due to the depletion of chloride through the reaction of gaseous hydrochloric acid with SS (Newberg et al., 2005).

POM was calculated using OM/OC ratios to account for additional species associated with OC. Previous work by Hand et al. (2019) suggested that a constant OM/OC ratio of 1.8 applied to IMPROVE OC data was contributing to biases in the fine mass residual, defined as the difference between gravimetric PM$_{2.5}$ mass and reconstructed fine mass (RCFM). RCFM is the sum of the species listed in Table 1. Gravimetric fine mass and RCFM should agree if sampling assumptions used to calculate RCFM are appropriate and measurement biases are low. However, the residual had increased since 2005 and was found to vary seasonally. An increase in the residual over time suggested either an increase in biases associated with gravimetric PM$_{2.5}$ mass, or an underestimation of RCFM, or both. A multiple linear regression (MLR) analysis indicated that the constant OM/OC ratio of 1.8 used to calculate POM was likely too low during warm months, resulting in an underestimate of RCFM that contributed to the seasonal bias in the residual (Hand et al., 2019). Monthly OM/OC values were derived using an MLR performed on monthly aggregated data from 2016 through 2019 (Hand et al., 2023) and are reported in Table 2. These derived OM/OC ratios are consistent with values reported in other studies in rural areas (e.g., Blanchard et al., 2016; El-Zanan et al., 2005, 2009; Hallar et al., 2013; Lowenthal et al., 2009, 2015; Malm et al., 2011, 2020; Malm & Hand, 2007; Ruthenburg et al., 2014; Simon et al., 2011). Using monthly OM/OC ratios to calculate POM at all IMPROVE sites reduced the network 2016–2019 annual average residual from 0.17 μg m^{-3} (using an OM/OC of 1.8) to 0.05 μg m^{-3}. To compute POM using urban CSN data, estimates from Philip et al. (2014) were applied to OC data for warm and cold months (Table 2).

For both networks, monthly and annual mean data at each site were aggregated from 2019 through 2022. Completeness criteria were applied similarly to data from both networks, resulting in 157 IMPROVE sites and 128 CSN sites used in the analysis. Fifty percent completeness of the data (2 years of valid monthly mean data) for a given site was required to be included in the analysis, with half of the daily observations in each month required for a valid

Table 2

OM/OC Ratios Used to Calculate Particulate Organic Mass (POM) for the IMPROVE Network and the CSN

Month	IMPROVE	CSN
Jan	1.5	1.6
Feb	1.5	1.6
Mar	1.5	1.6
Apr	1.6	1.6
May	1.7	1.6
Jun	1.9	1.8
Jul	2.0	1.8
Aug	2.1	1.8
Sept	2.0	1.8
Oct	1.7	1.8
Nov	1.7	1.8
Dec	1.7	1.8

monthly mean. Annual means were calculated from monthly means and required two out of three valid monthly means in each season, with seasons defined as winter (December, January, February), spring (March, April, May), summer (June, July, August), and fall (September, October, November). These criteria were applied consistently for each species. Average RCFM calculations were performed by summing the monthly and annual means of individual species; for example, average concentrations of each species were computed and summed to obtain an average RCFM. Valid data for all the species (i.e., AS, AN, POM, EC, FD, and SS) were required to compute monthly and annual mean RCFM. The monthly and annual mean fractional contribution (mass fraction) of each species to RCFM was also determined.

IMPROVE and CSN data were regionally aggregated according to previously defined regions based on site location and the seasonal distribution of aerosol concentrations for major species (Hand, Schichtel, & Pitchford et al., 2012; Hand et al., 2013; Malm et al., 2004). The variability in the composition between sites within a given region was not accounted for, nor were differences in site elevation. Of the 26 IMPROVE rural regions, two regions had only one site. The IMPROVE sites and regions that met completeness criteria are listed in Table S1 of Supporting Information S1. Twenty nine CSN regions were the same as defined in previous studies (Hand, Schichtel, & Pitchford et al., 2012; Hand et al., 2023). Ten CSN regions had only one site per region. A list of the CSN sites that met the completeness criteria and associated regions is provided in Table S2 of Supporting Information S1. The IMPROVE network has a higher site density in the western United States, while the CSN has a higher site density in the East.

2.3. Collocated Data Comparisons

The IMPROVE network and the CSN operate collocated samplers in several urban/suburban sites. Data from collocated sites were compared to identify relative biases between IMPROVE and CSN aerosol concentrations. Monthly mean data for AS, AN, OC, EC, FD, SS, FM, and RCFM were compared at Birmingham, Alabama; Fresno, California; Phoenix, Arizona; Puget Sound, Washington, Atlanta, Georgia, and Pittsburgh, Pennsylvania for 2019–2022. FM data for CSN were obtained from collocated FRM samplers corresponding to the same CSN sampling days. Scatter plots of monthly mean speciated mass concentrations for all six sites are presented in Figure 1.

A summary of comparison statistics is provided in Table 3. Biases were typically within ±16% for all species, except for a −34% bias in FD (IMPROVE higher) and 28% bias in EC (CSN higher). Errors were less than 20% for most species, except for FD (36%) and EC (31%). Errors were higher for EC due to different TOA hardware and analysis used for IMPROVE and CSN (Zhang et al., 2022) that resulted in higher EC concentrations for CSN filters. The correlation coefficient for EC was 0.88 and the ratio of average IMPROVE to average CSN concentrations was the lowest (0.81) of all the species. Higher biases and errors associated with FD may be due in part to differences in the sharpness of the cut points between IMPROVE and CSN samplers (Solomon et al., 2014), with sharper CSN cut points resulting in lower concentrations, presumably because less of the coarse tail of the FD size distribution is collected by the $PM_{2.5}$ filter. In addition, differences in the CSN and IMPROVE FD algorithms contributed to the bias; using the original FD algorithm for the IMPROVE data, the bias and error are −24% and 28%, respectively. The bias and error for SS was much lower than for FD. The lowest errors corresponded to AS, AN, and RCFM (<10%). Errors in FM (17%) were higher than RCFM (7% respectively), perhaps related to different face velocities associated with different samplers that could lead to losses of volatile species (Gorham et al., 2021; Malm et al., 2011; Solomon et al., 2014). Additional comparisons between IMPROVE and CSN collocated data are described by Gorham et al. (2021) and Kaur et al. (2024). The comparison statistics for the species listed in Table 3 were consistent with those reported for similar comparisons in 2005–2008 (for seven collocated sites, Hand, Schichtel, & Pitchford et al., 2012), with the exception of EC (higher biases in 2019–2022, for the reasons discussed above), and SS (lower biases in 2019–2022). CSN started reporting chloride ion data in 2017; in 2005–2008 SS for CSN was calculated with chlorine data from XRF.

3. Regional and Monthly Mean Mass Concentrations

The regional, monthly mean IMPROVE and CSN data are presented as stacked bar charts for both absolute and relative concentrations (mass fractions) in Figure 2 through Figure 7. IMPROVE regions are designated as "rural" in the discussion, although some sites are more remote than others, and CSN regions are designated as "urban" although some sites are in more suburban areas. Monthly mean concentrations are depicted with the first letter of
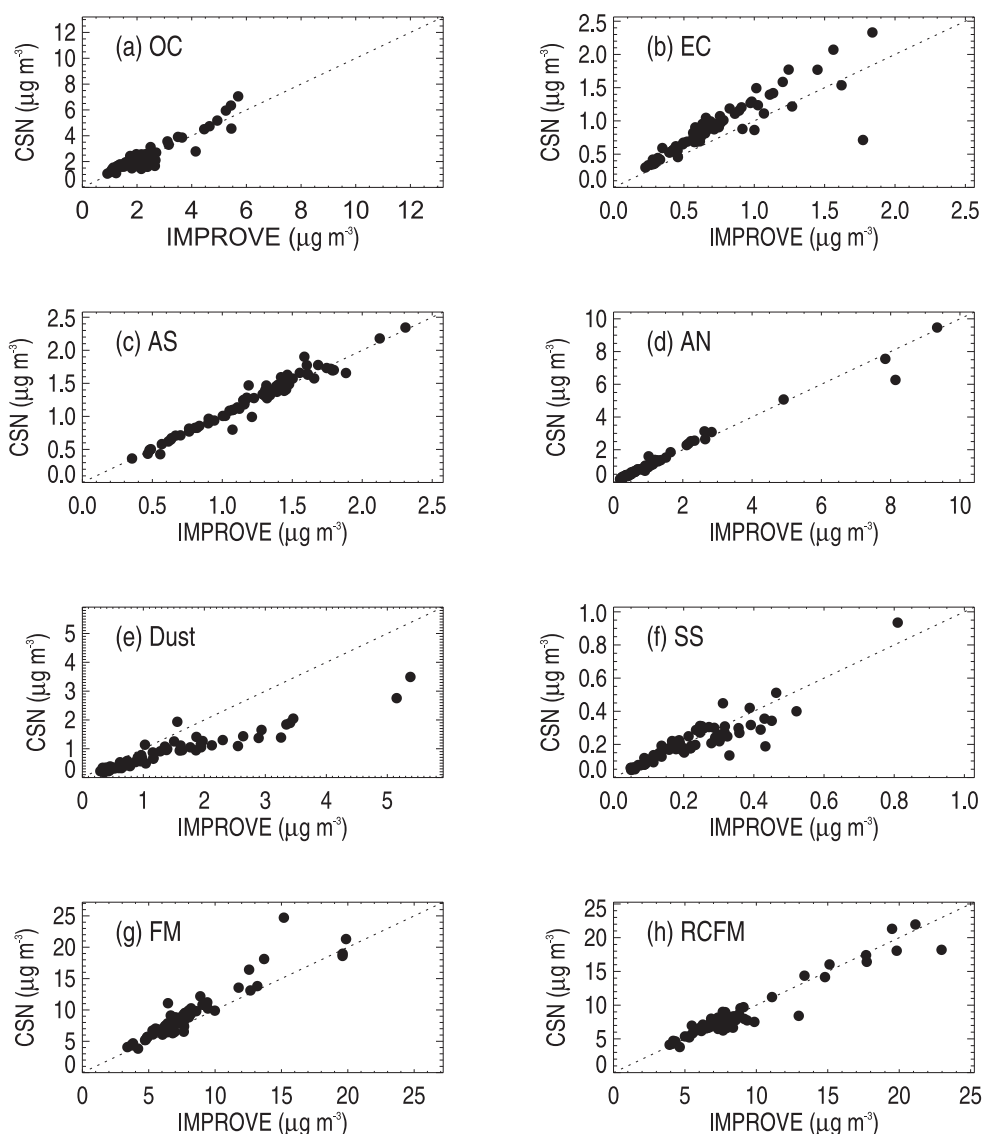
Figure 1. Comparisons of 2019–2022 monthly mean $PM_{2.5}$ aerosol mass concentration data (µg m^{-3}) for six collocated IMPROVE and CSN sites (see text) for (a) organic carbon (OC), (b) elemental carbon (EC), (c) ammonium sulfate (AS), (d) ammonium nitrate (AN), (e) fine dust, (f) sea salt (SS), (g) $PM_{2.5}$ gravimetric fine mass (FM), and (h) reconstructed fine mass (RCFM).

the month followed by an "A" for annual mean, with varying scales for each region. Regional bar charts are grouped and presented in three main areas: eastern, northwestern, and southwestern United States. The $PM_{2.5}$ species included in the bar charts are AS, AN, POM, EC, FD, and SS. Seasonality in each species is defined as the ratio of the maximum to minimum monthly mean concentration. Fine mass residuals (also referred to as "unidentified mass") are not included in these figures or analyses. Evaluating the fine mass residual is necessary for understanding biases in measurements and reconstruction algorithms but is outside the scope of this work (e.g., Hand et al., 2019). The following sections are organized by species.

3.1. Ammonium Sulfate

3.1.1. Absolute Concentration

The highest anthropogenic sources of SO_2 emissions in the United States are in the East (e.g., Hand et al., 2020) and lead to regional impacts of sulfate aerosols on $PM_{2.5}$. This regional impact is evidenced in similar

Table 3
Comparisons Between 2019 and 2022 Monthly Mean Data at Collocated IMPROVE and CSN Sites

Statistic	OC	EC	AS	AN	FD	SS	FM	RCFM
Annual average IMPROVE (µg m^{-3})	2.3	0.7	1.2	1.2	1.3	0.2	7.8	8.6
Annual Average CSN (µg m^{-3})	2.4	0.9	1.2	1.3	0.8	0.2	9.0	8.5
Bias[a] (%)	9	28	2	8	−34	−2	16	−0.2
Error[b] (%)	17	31	3	8	36	15	17	7
r	0.93	0.88	0.98	0.99	0.95	0.90	0.93	0.96
IMP/CSN	0.94	0.81	0.98	0.97	1.60	1.06	0.87	1.02

Note. Species include organic carbon (OC), elemental carbon (EC), ammonium sulfate (AS), ammonium nitrate (AN), fine dust (FD), sea salt (SS), PM$_{2.5}$ gravimetric fine mass (FM), and PM$_{2.5}$ reconstructed fine mass (RCFM). Positive biases correspond to higher CSN concentrations. [a]Bias (%) $= 100 \times \frac{1}{N}\sum_1^N \frac{\overline{X}_i - \overline{Y}_i}{\overline{Y}_i}$ and $\overline{X}_i$ and $\overline{Y}_i$ are the monthly mean data for CSN and IMPROVE concentrations for all six sites, respectively. N gives the number of data points (72). [b]Error (%) $= 100 \times \text{median}\left(\left|\frac{\overline{X}_i - \overline{Y}_i}{\overline{Y}_i}\right|\right)$.

concentrations of AS in eastern urban and rural regions. The maximum rural regional monthly mean AS concentrations in the East ranged between ∼0.9 and 1.9 µg m^{-3} (Figure 2). The highest monthly mean rural concentrations (1.9 µg m^{-3}) occurred in the Ohio River Valley and Midsouth regions in summer. Urban regional maxima were also around 2 µg m^{-3} (Figure 3), although three regions had maximum concentrations greater than 2 µg m^{-3}, with the highest in the East Texas/Gulf in April (2.6 µg m^{-3}) and the urban Ohio River Valley region in July (2.3 µg m^{-3}). Both rural and urban maxima have decreased dramatically since the earlier study in 2005–2008 (Hand, Schichtel, & Pitchford et al., 2012), when the maxima in the rural and urban Ohio River Valley regions were 9.5 µg m^{-3} and 10.3 µg m^{-3}, respectively. This decrease reflects the strong reduction in sulfate concentrations in the eastern United States, especially during summer due to the significant reduction of SO$_2$ emissions (Cheng et al., 2024; Hand et al., 2024). The lowest rural regional, monthly mean AS concentrations ranged from 0.5 to 1.1 µg m^{-3}, and the lowest urban mean concentrations ranged from 0.8 to 1.6 µg m^{-3}. The lowest minimum monthly mean concentrations occurred in the rural and urban Northeast regions in October (0.5 µg m^{-3} and 0.8 µg m^{-3}, respectively).

Monthly mean AS concentrations in regions in the northwestern United States were lower than in the eastern United States for rural regions (typically <1 µg m^{-3}) and urban regions (<∼1.4 µg m^{-3}), as seen in Figures 4 and 5, respectively. The highest mean AS concentrations (1.0 µg m^{-3} and 1.4 µg m^{-3}) occurred in the rural Northern Great Plains region and urban North Dakota region, both in February. Earlier studies have suggested the impacts of oil and gas development on PM in this region, especially in winter (Gebhart et al., 2018; Hand, & Gebhart et al., 2012; Prenni et al., 2016). Maxima for most other rural and urban northwestern regions occurred in summer months (Figures 4 and 5, respectively). AS concentrations in the northwestern regions have not decreased as much as in eastern regions (Hand et al., 2024). By comparison, the maxima for the rural Northern Great Plains and urban North Dakota region in 2005–2008 were 1.5 µg m^{-3} and 2.0 µg m^{-3}, respectively, both in spring months, and Hand et al. (2024) showed that sulfate decreased more during spring than summer months in this region. The minimum mean AS concentrations were much lower than in the East; the lowest occurred in both the rural and urban Northwest regions (0.10 µg m^{-3} and 0.4 µg m^{-3}, respectively), both in January. Most of the lowest mean AS concentrations occurred during cold months. The maximum monthly mean urban AS concentration for all U.S. urban regions occurred in Alaska in January (4.9 µg m^{-3}, see Figure 5), compared to the maximum rural Alaska mean concentration of 0.6 µg m^{-3} in April (Figure 4). The higher 2005–2008 rural Alaska maximum (0.9 µg m^{-3}) also occurred during spring. AS concentrations in Alaska in spring have decreased stronger than during other seasons (Hand et al., 2024).

AS regional, monthly mean concentrations in the southwestern regions were similar or greater in magnitude to monthly mean concentrations in eastern regions for both rural and urban regions (Figures 6 and 7, respectively). Sources of sulfate in the East are associated with electric generating units, which are fewer in the West (Hand, Schichtel, & Malm et al., 2012). The highest urban monthly mean AS concentration in the southwestern United States occurred in the Los Angeles region (4.0 µg m^{-3}) in July, where potential sources include oxidation of

Figure 2. Rural IMPROVE 2019–2022 regional, monthly mean speciated PM$_{2.5}$ mass concentrations (μg m^{-3}), and mass fractions for the eastern United States, including the Virgin Islands region. The letters on the *x*-axis correspond to month, with the annual mean denoted as "A." The shaded areas correspond to regions, with sites shown as dots.

Figure 3. Urban CSN 2019–2022 regional, monthly mean speciated PM$_{2.5}$ mass concentrations (µg m^{-3}), and mass fractions for the eastern United States. The letters on the x-axis correspond to month, with the annual mean denoted as "A." The shaded areas correspond to regions, with sites shown as dots.
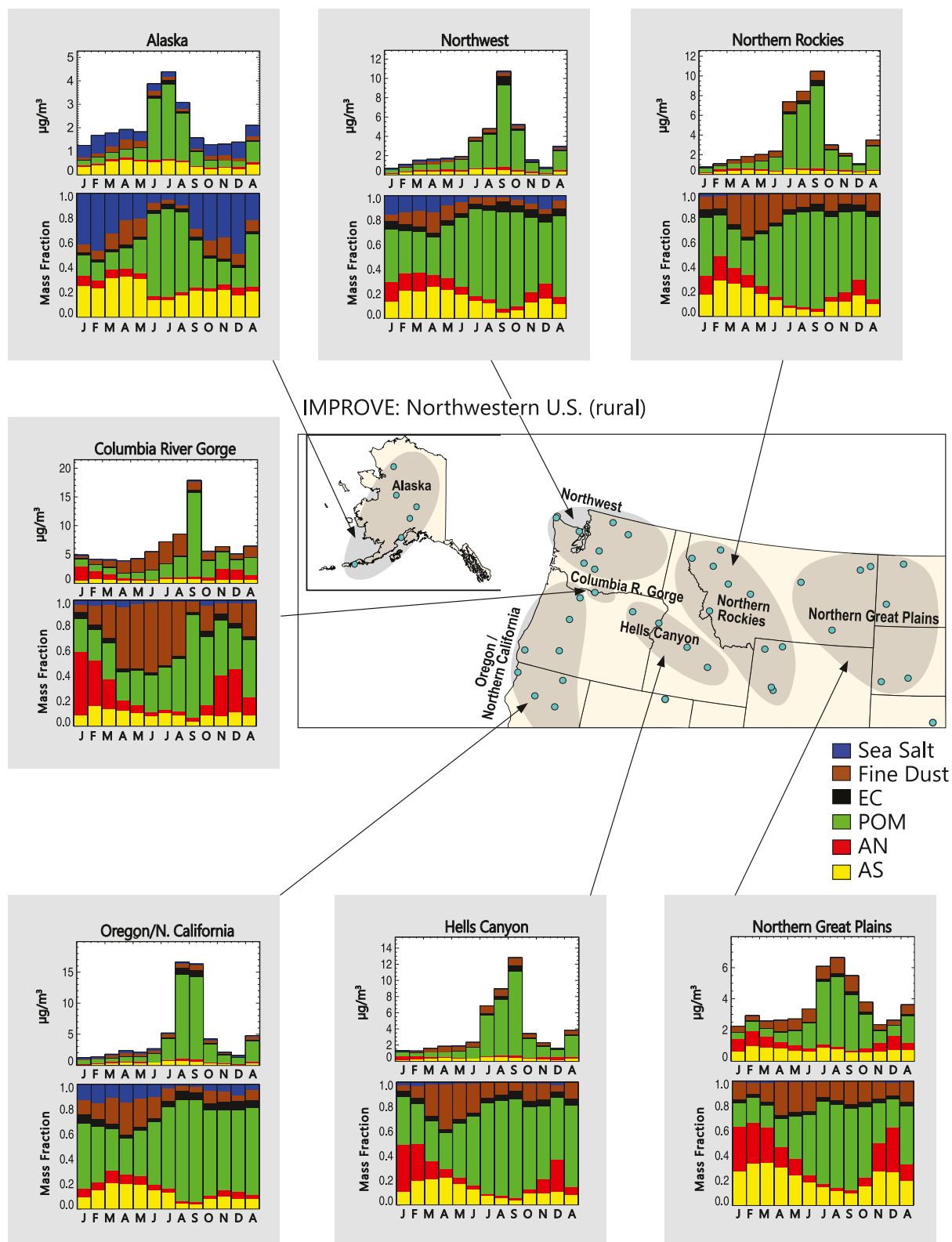
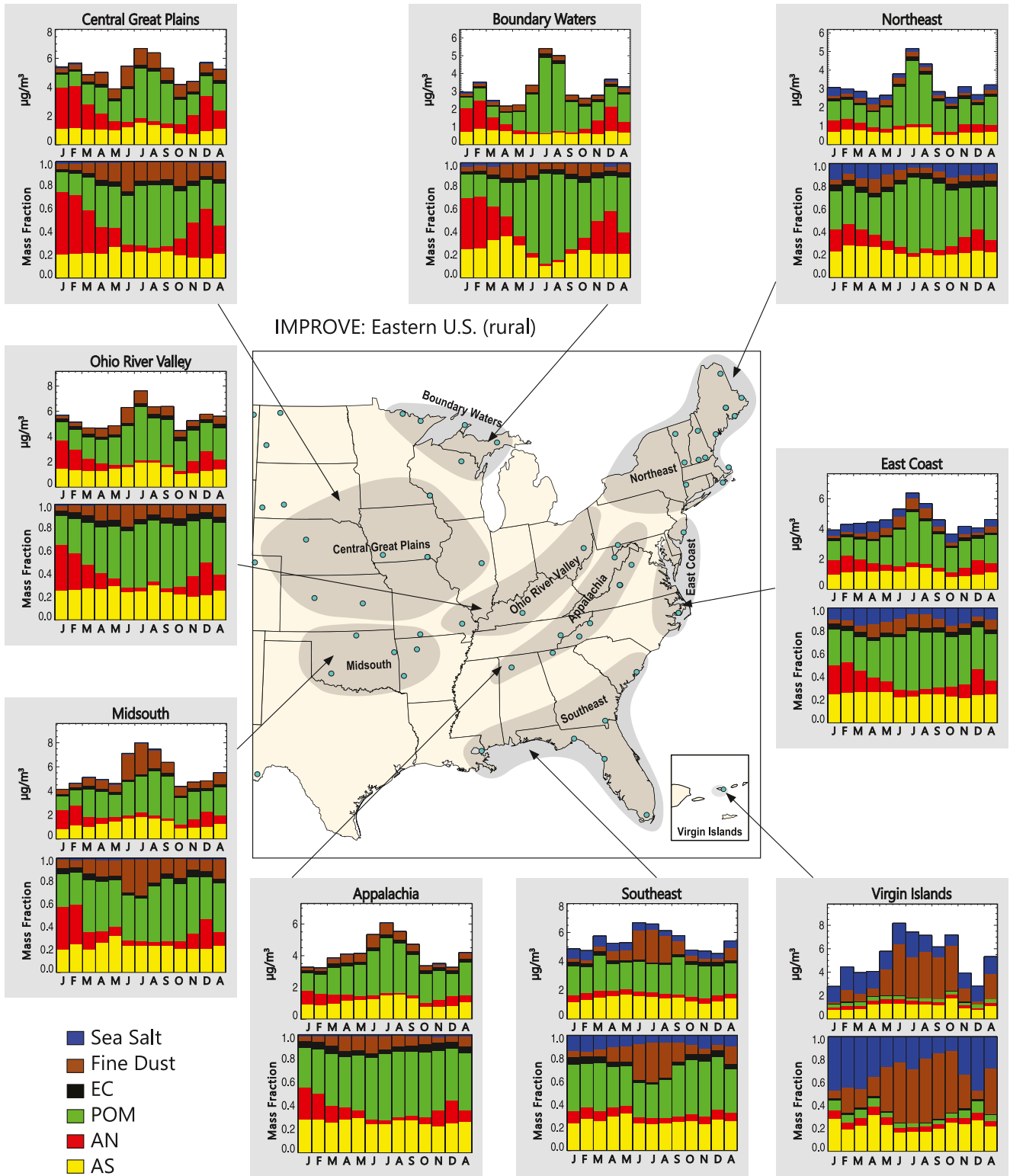**Figure 4.** Rural IMPROVE 2019–2022 regional, monthly mean speciated PM$_{2.5}$ mass concentrations (μg m^{-3}), and mass fractions for the northwestern United States, including the Alaska region. The letters on the *x*-axis correspond to month, with the annual mean denoted as "A." The shaded areas correspond to regions, with sites shown as dots.
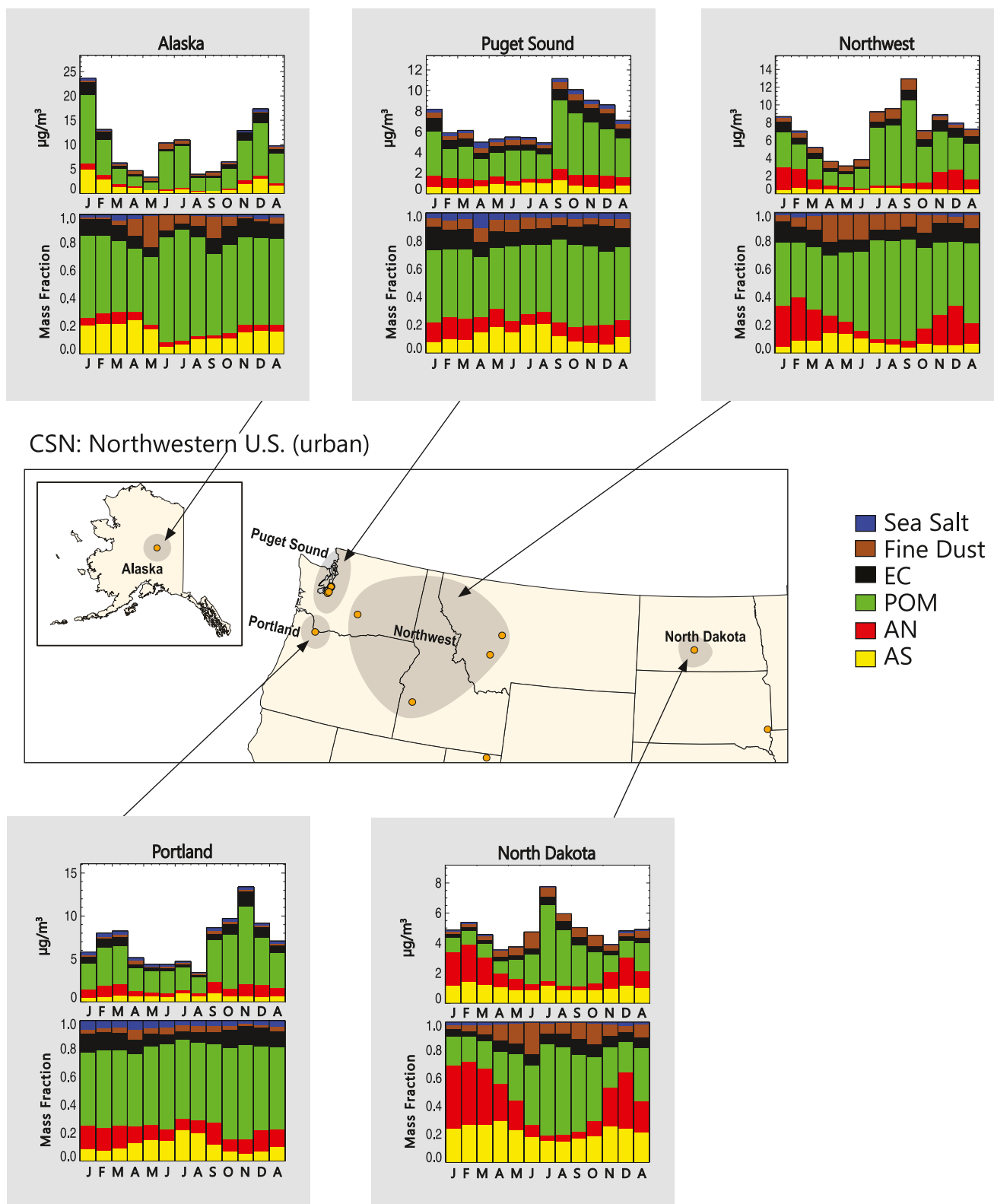
Figure 5. Urban CSN 2019–2022 regional, monthly mean speciated PM$_{2.5}$ mass concentrations (µg m^{-3}), and mass fractions for the northwestern United States, including the Alaska region. The letters on the *x*-axis correspond to month, with the annual mean denoted as "A." The shaded areas correspond to regions, with sites shown as dots.
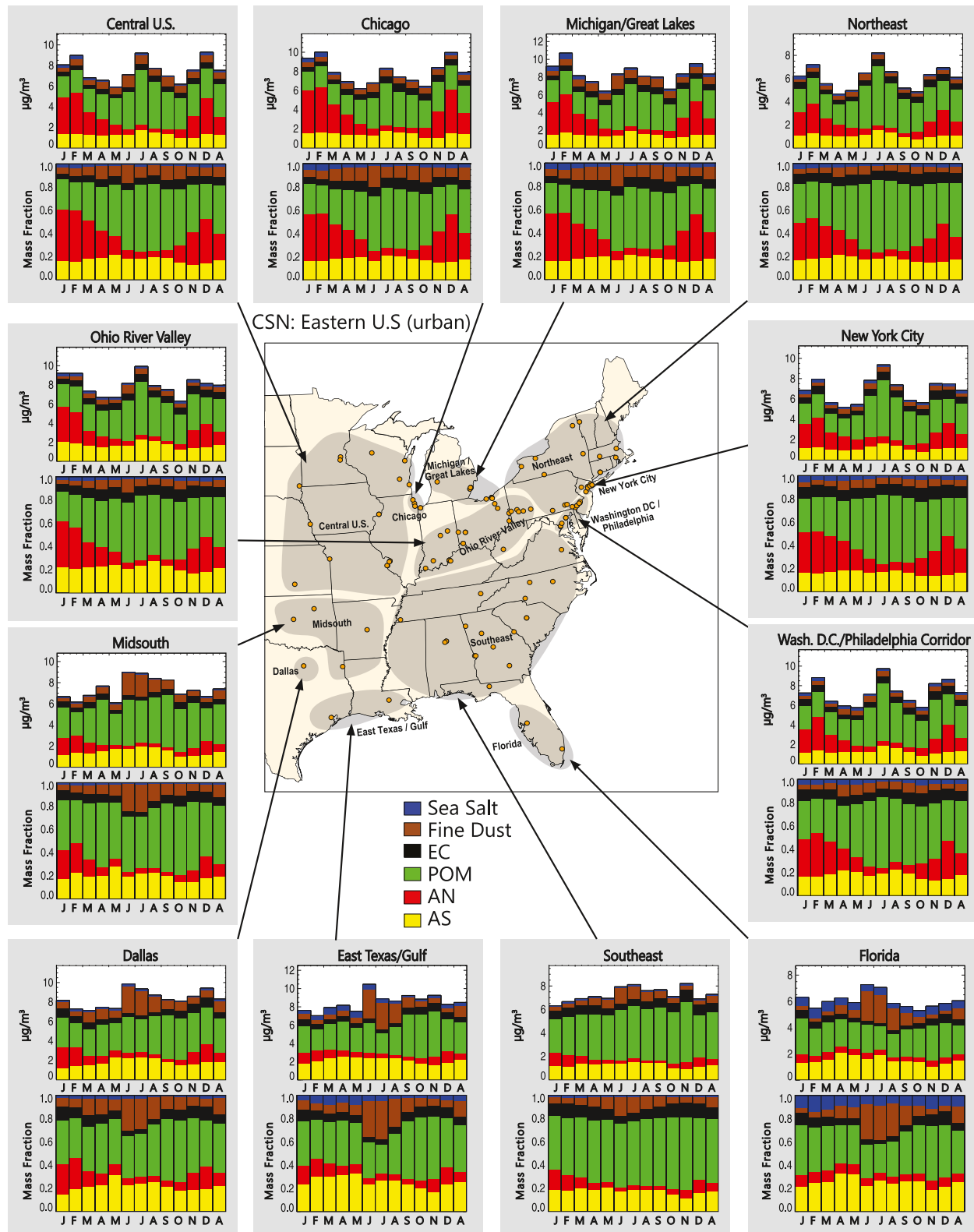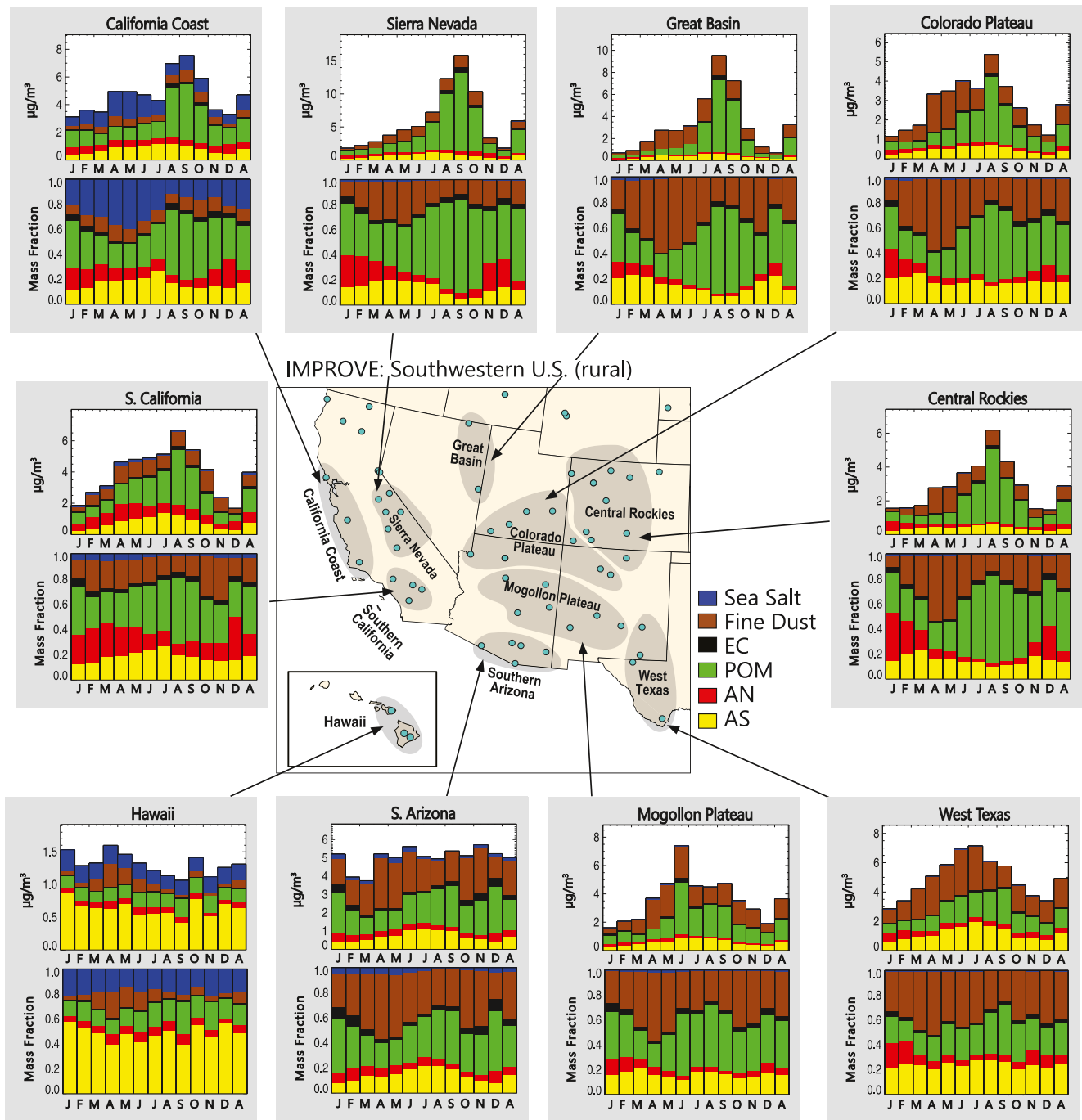
Figure 6. IMPROVE 2019–2022 regional, monthly mean speciated PM$_{2.5}$ mass concentrations (μg m^{-3}), and mass fractions for the southwestern United States, including the Hawaii region. The letters on the *x*-axis correspond to month, with the annual mean denoted as "A." The shaded areas correspond to regions, with sites shown as dots.

anthropogenic emissions (Hersey et al., 2013) and shipping (Ault et al., 2010). The maximum rural monthly mean of 2.0 μg m^{-3} occurred in the West Texas region in July (Figure 6). These maxima have decreased in both the urban Los Angeles and rural West Texas regions since 2005–2008 (previous values of 7.0 μg m^{-3} in July, and 3.0 μg m^{-3} in June, respectively). Nearly all the rural southwestern regions had maximum AS concentrations during summer months (July and August), as did the urban regions, except for the urban Front Range, CO region in February (1.1 μg m^{-3}). Minimum monthly mean concentrations (~0.2 μg m^{-3}) occurred during winter months.

Figure 7. Urban CSN 2019–2022 regional, monthly mean speciated PM$_{2.5}$ mass concentrations (μg m^{-3}) and mass fractions for the southwestern United States, including the Hawaii region. The letters on the *x*-axis correspond to month, with the annual mean denoted as "A." The shaded areas correspond to regions, with sites shown as dots.
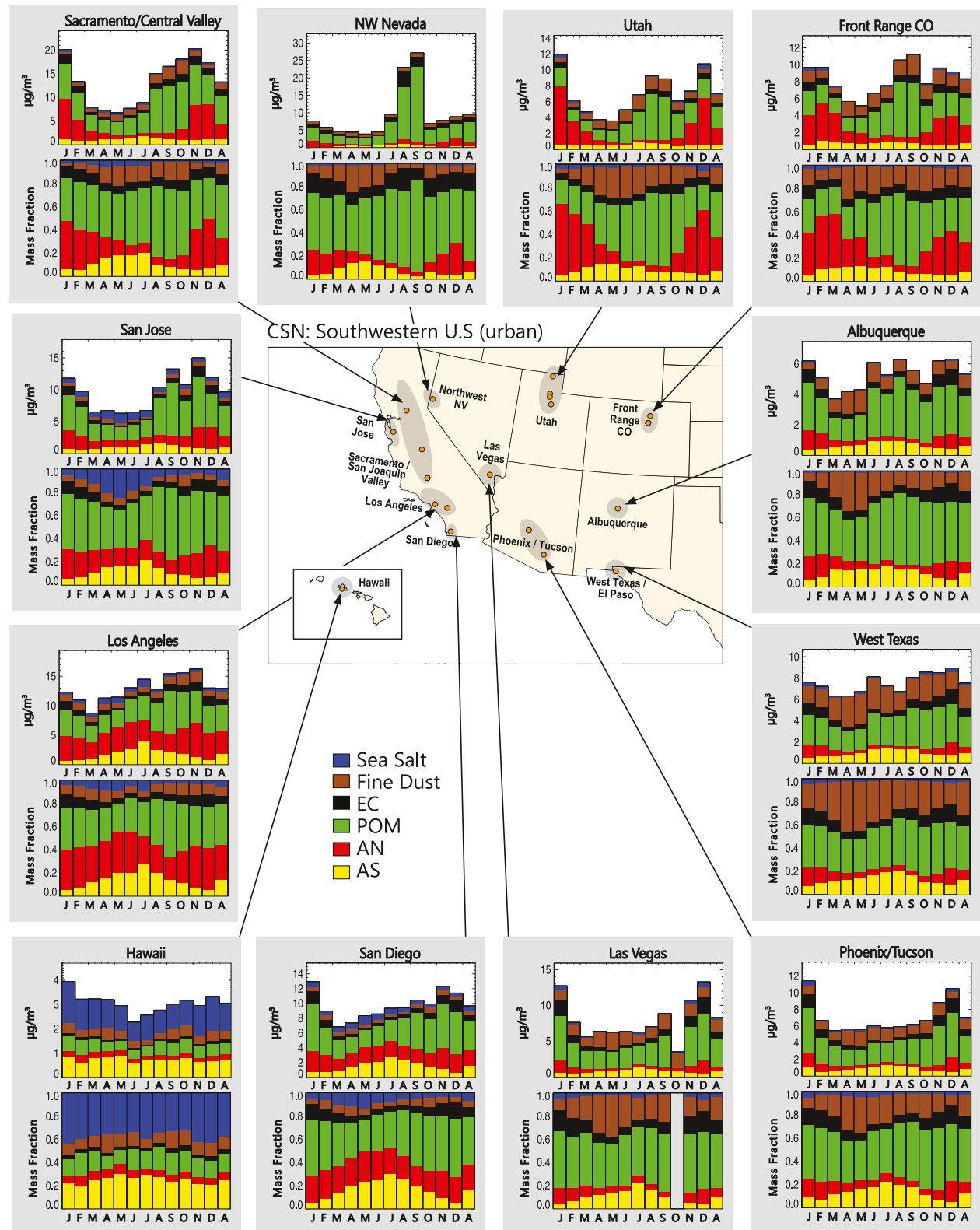
In the Hawaii region, urban and rural maxima were 0.9 µg m^{-3}. The rural Hawaii region is known to be influenced by volcanic emissions (Hand et al., 2024).

3.1.2. Relative Concentration

Urban and rural regional, maximum monthly mean mass fractions of AS were around 0.3 for nearly all regions, meaning that on average, AS contributed a monthly mean maximum of around 30% to RCFM across the United States. In nearly all regions of the United States, AS is no longer the major contributor to RCFM. Contributions from AS to RCFM have strongly decreased since 2005–2008 when maximum mean AS contributions were typically 60% in summer at urban and rural regions in the eastern United States, and around 20% in western regions. In the eastern United States, the 2019–2022 maximum rural monthly mean contribution to RCFM of 36% occurred in the Boundary Waters region in April (Figure 2), compared to the urban maximum of 33% in the East Texas/Gulf region in May (Figure 3). For both rural and urban eastern regions, the maximum AS contribution occurred most often in spring or summer months. Minimum mean contributions were around 11% in eastern urban and rural regions. In the northwestern United States, the maximum mean contribution was similar to contributions in the East, with a high of 34% in the rural Northern Great Plains in March, and 29% in the urban North Dakota region in April (Figures 4 and 5, respectively). Minimum mean contributions in urban and rural regions were less than 5%. In the southwestern United States, the minimum and maximum mean contributions ranged from 3% to ∼30%, respectively, for rural and urban regions (Figures 6 and 7, respectively), with the highest in the urban San Diego region and the rural West Texas region in summer. The minimum mean contributions were less than (5%). As seen in Figure 6, AS was the dominant contributor to RCFM in the rural Hawaii region, with contributions ranging from 40% to 58%, respectively, compared to 20%–30% from the 2005–2008 study period.

3.1.3. Seasonality

The seasonality of AS in the eastern United States has significantly decreased over the past decades due to stronger reductions in summer AS concentrations because of reductions in emissions and oxidant availability (Chan et al., 2018; Hand et al., 2024; Shah et al., 2018). For eastern regions, the monthly mean AS seasonal ratio (ratio of maximum to minimum monthly mean concentration) in urban and rural AS was generally less than two, meaning that the maximum monthly mean concentration was less than twice the minimum, with an eastern average seasonal ratio of 1.9 in both urban and rural regions. For 2005–2008, the eastern average was 2.4 and 2.6 for urban and rural regions, respectively. The strongest decrease in AS seasonality occurred in the rural Appalachian region, where the seasonal ratio decreased from four to two over the past two decades.

AS had a much higher degree of seasonality in the rural northwestern regions compared eastern United States. The average seasonal ratio for all rural northwestern regions was 3.9, with the highest degree of seasonality in the Northwest and Oregon/Northern California regions (∼6.0). The average seasonal ratio in urban northwestern regions was ≤2. In the southwestern United States, the strongest seasonality in AS occurred in the rural Southern California region (5.8) and the urban San Diego (6.6) and Los Angeles regions (5.9). Other southwestern urban and rural regions had lower seasonality (3–4). The urban Alaska region had the highest degree of AS seasonality of any region (12), with a winter maxima and summer minimum, compared to the rural region (2.6) with a spring maximum and winter minimum. Air quality in the urban Alaska region (i.e., Fairbanks) often exceeds PM$_{2.5}$ standards during winter due to local emissions that are trapped near the surface during inversions (Robinson et al., 2024).

3.2. Ammonium Nitrate

3.2.1. Absolute Concentration

In the eastern United States, regional mean AN concentrations peaked in winter months for all urban and rural regions (Figures 2 and 3, respectively). Concentrations were higher in urban regions, with a maximum urban mean AN concentration of 4.8 µg m^{-3} in the Chicago region compared to the 2.9 µg m^{-3} in the Central Great Plains region, both in winter. In 2005–2008, the maximum mean AN concentration in the Chicago region was 7.1 µg m^{-3} and in the rural Central Great Plains was 4.1 µg m^{-3}. AN concentrations have decreased in winter in this region over the past two decades at a rate of around −2% yr^{-1} (Hand et al., 2024). Lower AN concentrations were observed farther south and distant from agricultural sources in the central United States (e.g., Heald

et al., 2012; Pitchford et al., 2009). For example, the maximum mean AN concentrations in the rural and urban Southeast regions (both in January) were 0.5 μg m^{-3} and 1.1 μg m^{-3}, respectively.

In the northwestern United States, the regional, maximum AN mean concentrations were lower than in East. The urban and rural maximum was the same (2.5 μg m^{-3}) in the rural Columbia River Gorge region (Figure 4) and the urban Northwest region (Figure 5), both in January. AN peaked in winter for all the urban regions in the northwestern United States. Most rural regions also had winter maxima, except for the Oregon/Northern California region in August (0.4 μg m^{-3}) and the Northwest region in September (0.3 μg m^{-3}). These maxima may have been influenced by biomass smoke impacts (Figure 4) as AN and POM peaked on the same days at several sites in the region (e.g., Benedict et al., 2017; Lindaas et al., 2021). In general, in the northwestern United States, urban mean AN concentrations were greater than rural mean concentrations, with all urban regions having maxima greater than 1 μg m^{-3} and nearly rural regions with maxima less than 1 μg m^{-3}.

The highest maximum monthly mean urban AN concentrations in all regions of the United States occurred in the southwestern regions of Sacramento/Central Valley (8.4 μg m^{-3}) and Utah (7.4 μg m^{-3}), both in January (Figure 7). Both maxima were considerably lower than the 2005–2008 values (14.09 μg m^{-3} and 11.42 μg m^{-3}, respectively). Some of the largest decreases in rural AN concentrations in the United States occurred in California (Figure 6), likely due to reductions in NO$_x$ emissions (Hand et al., 2024; Russell et al., 2012; Tong et al., 2015; Yu, McDonald, & Harley, 2021). All the southwestern urban regions had maxima over 1 μg m^{-3} during cold months. Rural AN mean concentrations were much lower than in urban regions, with mean maximum concentrations less than 1 μg m^{-3}, with the exception of the Southern California region (1.1 μg m^{-3} in April). Other rural maxima occurred during winter months except the Great Basin region in August and the Mogollon Plateau region in June. Both regions may have been influenced by emissions from biomass smoke, as POM was also high during these months and both AN and POM peaked on similar days at some sites (Figure 6).

3.2.2. Relative Concentration

During winter months in the eastern United States, AN was responsible for half of the RCFM at regions farther north (Figure 2). The maximum eastern contributions occurred at the rural Central Great Plains (54%) and the urban Chicago (48%) regions, and many eastern regions had contributions around 40%–50% during winter months. These contributions were similar to the 2005–2008 period (~50%). At southern regions in the East, such as the rural and urban Southeast regions, maximum contributions were on the order of 10%–20% and peaked during winter months (Figures 2 and 3, respectively). In the northwestern United States contributions from AN were around 50% for both rural and urban regions (Figures 4 and 5, respectively). The highest AN mean contribution in the northwestern United States occurred in the rural Columbia River Gorge region (50%) and the urban North Dakota region (46%), both in January. Contributions in other rural northwestern regions, such as the Oregon/Northern California, Northern Rockies, and Northwest regions were <20%, as were the contributions at the urban Puget Sound and Portland regions during winter months. The largest urban/rural differences in AN contributions occurred at regions in the southwestern United States. Contributions in rural regions were typically <20% (Figure 6), except for the rural Southern California region (38% in December). Most of the urban regions had maximum contributions over 20% (Figure 7), with the largest in the urban region of Utah (61% in January). Several urban regions had contributions around 40% or greater, including the Sacramento/Central Valley, Los Angeles, and Front Range CO regions. Minimum monthly mean contributions in urban and rural southwestern regions were on the order of 2%–4%. Maximum contributions in urban and rural Alaska and Hawaii regions were less than 10%.

3.2.3. Seasonality

AN had some of the highest seasonality of any species. In the eastern United States, the average rural seasonal ratio was 8.0. The largest rural seasonal ratio occurred in the Boundary Waters region (19.8), similar to 2005–2008 (20.0). The 2019–2022 seasonal ratio in the rural Ohio River Valley region increased since 2005–2008 (12.9 compared to 8.5, respectively). Urban AN seasonality in the eastern United States was lower than for rural regions, with an eastern average ratio of 6.3, although several regions had seasonal ratios greater than 8. The urban Ohio River Valley region also increased in seasonality compared to 2005–2008 (9.1 vs. 5.1, respectively). In the northwestern United States, the rural seasonality in AN was largest in the Columbia River Gorge region (13.1) and increased since 2005–2008 (5.1). The urban Northwest region (12.4) and North Dakota region (9.7)

AN also had strong seasonal variability. The lowest rural AN seasonality in the United States occurred for regions in the southwestern United States, with ratios around 3, except for the rural Central Rockies (5.1). The highest seasonality in AN in all urban regions occurred in the Utah region (26.0). The urban Northwest Nevada and Central Valley regions both had seasonal ratios around 11–12, contrasting regions in southern California that had lower seasonal ratio (∼2), such as the Los Angeles and San Diego regions.

3.3. POM

3.3.1. Absolute Concentration

One of the most significant changes in aerosol composition in the United States corresponds to the shift from a sulfate-dominated to carbon-dominated fine mass. While OC has declined in many regions and seasons, it has not declined as quickly as sulfate (Hand et al., 2024; Malm et al., 2017). The rural eastern maximum monthly mean POM concentration (4.2 $\mu g\ m^{-3}$) in the Boundary Waters and Ohio River Valley regions was comparable to the combined maximum mean AN and AS concentrations (Figure 2). Most rural regions had maximum POM concentrations around 3 $\mu g\ m^{-3}$ that peaked in summer months when biogenic OC concentrations are highest (Schichtel et al., 2017). In 2005–2008, the maximum POM concentration (5.8 $\mu g\ m^{-3}$) occurred in the Southeast. Urban maximum regional mean POM concentrations were greater than rural regions (Figure 3). The highest maximum occurred in the Washington D.C./Philadelphia region (5.9 $\mu g\ m^{-3}$) and the New York City region (5.6 $\mu g\ m^{-3}$). Nearly all urban maxima occurred in summer months (Figure 3). The rural minimum mean POM concentration was considerably less than the urban minimum (rural Boundary Waters region was 0.6 $\mu g\ m^{-3}$ in March) compared to 1.7 $\mu g\ m^{-3}$ in the urban Northeast region in April.

The highest rural maximum mean POM concentrations occurred in the northwestern United States (Figure 4) in regions influenced by biomass smoke emissions, such as the Columbia River Gorge region (14.4 $\mu g\ m^{-3}$) in September and the Oregon/Northern California region (13.4 $\mu g\ m^{-3}$) in August due to high fire activity during this period (Childs et al., 2022; Dong et al., 2022; Hand et al., 2024; Prein et al., 2022; Safford et al., 2022; Xue et al., 2021). In 2005–2008, the rural maximum POM mean concentrations were 3.6 $\mu g\ m^{-3}$ and 5.4 $\mu g\ m^{-3}$ in the Columbia River Gorge and Oregon/Northern California regions, respectively, three to four times lower than current maxima. Unlike in winter and spring, OC temporal trends in the northwestern regions in summer and fall were positive and statistically insignificant (Hand et al., 2024). Monthly mean maxima in other rural regions (∼5–10 $\mu g\ m^{-3}$) occurred in late summer and early fall months. Urban mean maximum POM concentrations in the northwestern United States were lower than rural regions but also influenced by biomass smoke (Childs et al., 2022; Wilmot et al., 2021; Xue et al., 2021). The maximum urban mean concentration occurred in the Northwest region (9.4 $\mu g\ m^{-3}$) in September and the Portland region (9.0 $\mu g\ m^{-3}$) in November (Figure 5).

Biomass smoke also influenced some regions in the southwestern United States (Figures 6 and 7). The maximum mean concentrations occurred in late summer/early fall in the urban Northwest Nevada region (21.5 $\mu g\ m^{-3}$), rural Sierra Nevada region (11.7 $\mu g\ m^{-3}$), and the rural Great Basin region (6.5 $\mu g\ m^{-3}$). Like the northwestern regions, seasonal mean temporal trends in OC in the southwestern United States were negative in winter and spring, while trends in summer were flat and statistically insignificant due to smoke impacts (Hand et al., 2024). For example, the maximum POM mean concentration in the Sierra Nevada region in 2005–2008 was 5.1 $\mu g\ m^{-3}$, roughly half of the current maxima. In other southwestern regions, maximum mean rural concentrations were around 2–3 $\mu g\ m^{-3}$ during summer and early fall months, and urban POM maximum mean concentrations were above ∼4 $\mu g\ m^{-3}$, especially in the urban Sacramento/Central Valley region (10.1 $\mu g\ m^{-3}$) in October. Several of the urban southwestern regions had maxima in winter months (San Diego, Las Vegas, Phoenix), as did the rural Southern Arizona region, perhaps due to residential wood combustion (e.g., Brown et al., 2016; Pope et al., 2017). Outside of fire season the winter minimum mean POM concentration in the rural Great Basin region was considerably lower (0.2 $\mu g\ m^{-3}$, see Figure 6).

3.3.2. Relative Contributions

POM was the dominant species contributing to RCFM in both urban and rural regions across the United States, with maxima ranging from 70% to 80% in rural regions and 60%–80% in urban regions. In the East, the maximum POM contribution occurred in the rural Boundary Waters region in July (78%), likely due to smoke impacts. In other eastern rural regions, the maximum POM contributions were typically over 50%, usually in the summer or early fall (Figure 2). The exception was a November maximum in the rural Southeast region (48%). November
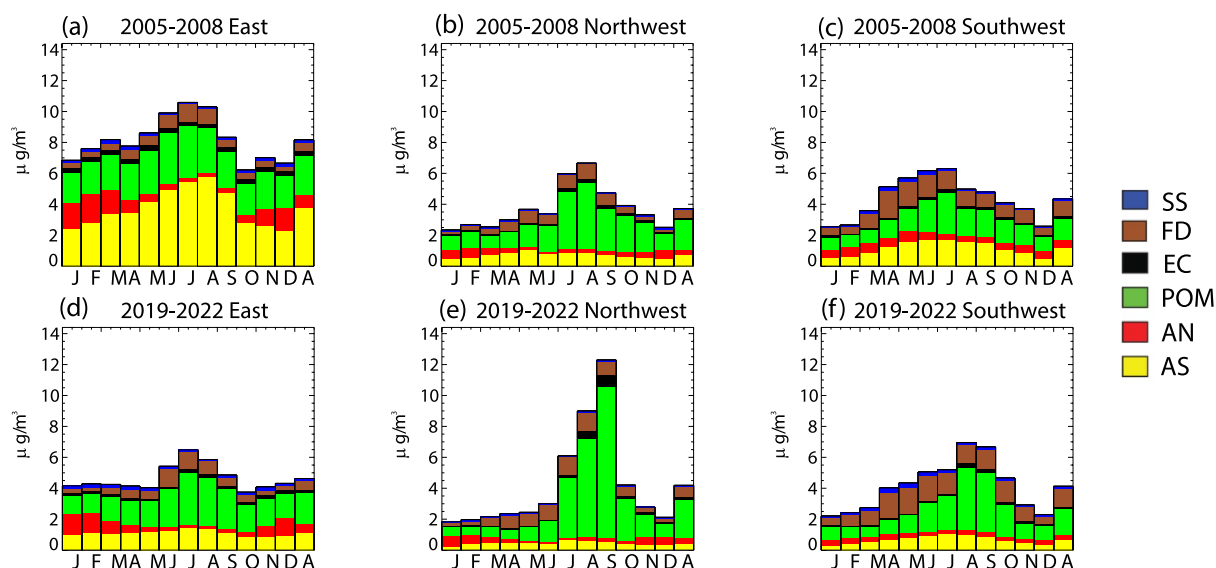
Figure 8. Rural IMPROVE area, monthly mean speciated PM$_{2.5}$ mass concentrations (μg m^{-3}) for 2005–2008 for the (a) East, (b) Northwest, Southwest and 2019–2022 for the (d) East, (e) northwest, and (f) southwest for ammonium sulfate (AS), ammonium nitrate (AN), particulate organic matter (POM), elemental carbon (EC), fine dust (FD), and sea salt (SS).

maxima also occurred in the urban eastern regions of Florida (48%) and the Southeast (62%). The urban Southeast region encompasses a larger geographical area than the rural region and contributions have increased from 47% in 2005–2008 (Figure 3). Maximum mean POM contributions in other urban eastern regions were around 50%–60% and most occurred in July or early fall months, similar to typical urban contributions across the East in 2005–2008. The highest contributions of POM to RCFM in the United States occurred in regions in the northwestern United States due to the influence of biomass smoke (Figure 4). All rural northwestern regions had maximum mean POM contributions over 70%, with the largest in the Columbia River Gorge region (82%) in September. The largest urban maximum POM contribution was somewhat lower (72%) in the Northwest region in September (Figure 5). In the Alaska region, the urban maximum contribution was 80% compared to rural contribution of 72%, both in July. However, in the Alaska region, urban contributions were over 50% year-round, whereas in the rural region contributions dropped to ∼15% in March. Biomass burning also likely led to large maximum mean contributions of POM in the Sierra Nevada region (74%) and the urban Northwest Nevada region (79%), both in September (Figures 6 and 7, respectively). Rural POM contributions decreased farther south, and maxima occurred in winter and late summer months, such as at the rural Southern Arizona region with maximum contributions (47%) in December. For urban regions in the southwestern United States, the maximum mean contributions occurred in either late summer/early fall or during cold months (e.g., San Diego, Las Vegas, Phoenix/Tucson, and West Texas), likely due to residential wood combustion (Figure 8). Minimum POM contributions at all U.S. urban and rural regions were around 10%–20%.

3.3.3. Seasonality

The seasonality of POM reflected the seasonal variability in OC as well as the OM/OC ratios used to calculate POM for both the IMPROVE and CSN data. POM seasonality was extreme depending on the region. In the eastern United States, its seasonal ratio was between that of AN and AS. The eastern maximum seasonal ratio occurred in the rural Boundary Waters region (7.1), compared to the highest urban seasonal ratio (3.2) in the New York City region. On average, the maximum monthly mean POM was 3.6 times larger than minimum in rural eastern regions, compared to 2.3 times higher in urban regions. Seasonal variability in the eastern regions increased for both rural and urban regions compared to 2005–2008 (previous values were 2.5 and 1.9, respectively). The seasonality in POM was high in rural northwestern regions due to the seasonal influence of biomass burning, with the largest seasonal ratio in the rural Northwest region (28.9). The average seasonal ratio in rural northwestern regions increased dramatically since 2005–2008 (20.5 vs. 7.2, respectively). The urban northwestern POM seasonality was lower compared to rural regions, with the highest seasonal ratio in the urban

Northwest region (6.1). Urban winter POM concentrations were higher than rural concentrations, indicating additional urban sources that led to less seasonality (Figure 5). Urban/rural differences in seasonality were also observed for regions in the southwestern United States. Some of the urban and rural regions farther north in this area had high seasonality, just as they had higher maximum POM concentrations, likely due to biomass smoke. For example, the rural Great Basin region had the largest seasonal ratio of any species and region in the United States (29.8), and the Sierra Nevada and Columbia River Gorge regions had seasonal ratios greater than 10 (Figure 6), as did the urban Northwest region (12.3). The seasonal ratio for rural regions southward was lower, near 2–7. This spatial trend also occurred for urban regions, but with much lower seasonality. The seasonality of other urban regions was flat (2–3), indicating additional urban sources, especially during winter (Figure 7). The seasonal ratio in the rural Alaska region was greater than the urban region (15.2 vs. 8.8, respectively) but with opposite maximum season, indicating additional winter urban sources of POM, likely associated with residential wood combustion (e.g., Busby et al., 2016; Robinson et al., 2024).

3.4. EC

3.4.1. Absolute Concentration

Urban mean EC concentrations were typically higher (>1.0 μg m^{-3}) than rural mean concentrations (<1.0 μg m^{-3}) due to additional urban sources, but also recall that collocated CSN EC concentrations were biased high (28%) relative to IMPROVE concentrations at collocated sites (Figure 1 and Table 3) due to differences in TOA hardware and analysis. The eastern regions had the lowest mean EC concentrations in the United States, with a rural maximum of 0.4 μg m^{-3} in the Ohio River Valley region in September, and urban maxima of 1.1 μg m^{-3} in the Dallas and Southeast regions, both in December (Figures 2 and 3, respectively). Rural mean EC concentrations in the East have declined significantly during all seasons (Hand et al., 2024), as observed in the decrease from the 2005–2008 rural maximum concentration of 0.5 μg m^{-3} in the rural Ohio River Valley region. The eastern urban regions had maximum mean EC concentrations mostly from August through December, but rural region maxima occurred during all months. The seasonal and spatial variability of EC suggested impacts from local sources in regions in the eastern United States (Hand et al., 2014).

The highest monthly mean rural EC concentrations in all U.S. regions occurred in the northwestern United States, not surprising given the wildfire impacts during this period (see Figures 4 and 5). The rural maximum mean EC (1.2 μg m^{-3}) occurred in the Northern California/Oregon region in August; all the rural maxima occurred in August and September (Figure 4). In 2005–2008, the rural maximum mean EC concentration was 0.3 μg m^{-3} in August in the Northern Rockies region. Like OC, EC trends in summer and fall in the northwestern United States were flat and statistically insignificant, likely due to impacts from biomass smoke (Hand et al., 2024) that impeded progress in anthropogenic EC reductions (e.g., Murphy et al., 2011). Urban maximum mean EC concentrations in the northwestern United States occurred in the Portland region in November (1.8 μg m^{-3}, Figure 5), similar in magnitude to the 2005–2008 urban maximum in the Northwest region (1.6 μg m^{-3}) in December. The urban Alaska region had a high EC maximum of 2.8 μg m^{-3} in January, compared to the rural Alaska maximum of 0.2 μg m^{-3} in July. EC monthly maxima that occurred during winter months suggested local sources of EC from residential wood combustion or meteorological conditions leading to inversions that trap urban sources (Robinson et al., 2024).

EC concentrations in southwestern regions were higher than in the eastern United States, and for urban regions, the highest maximum monthly mean EC concentrations occurred in the Northwest Nevada region in August (4.6 μg m^{-3}), likely associated with biomass burning as the maximum urban POM occurred in this same region in September (Figure 7). The highest maximum EC mean concentration for rural southwestern regions (0.9 μg m^{-3}) occurred in the Sierra Nevada region in September. The 2005–2008 maximum EC concentration in the Sierra Nevada region was 0.4 μg m^{-3} (July), reflecting positive and statistically insignificant trends during summer and fall (Hand et al., 2024). Most of the southwestern urban regions had maxima in winter months, while all the rural regions had maxima in summer/early fall months except for the Southern Arizona region (0.5 μg m^{-3} in December). Minimum EC mean concentrations for all rural regions were less than 0.1 μg m^{-3} and urban minima were around 0.2 μg m^{-3}.

3.4.2. Relative Concentration

EC maximum contributions to RCFM were typically 10% or less in both urban and rural regions. In the eastern United States, the maximum mean EC contribution (7%) occurred in March in the rural Appalachia region, with maximum values around 5% for other regions and minimum mean contributions around 2% (Figure 2). The maximum contribution in urban regions was 13% in the Southeast region in December (Figure 3). Most urban regions had maximum contributions around 10% and mostly during winter months, while minima were around 4%. The maximum rural contribution in the northwestern United States occurred at the Northwest region (9%) in September, similar to when the maximum POM contribution occurred (Figure 4). However, most of the rural northwestern maximum EC contributions occurred during winter months, and minima (∼3%) occurred during spring and early summer months. The urban maximum contributions in this area were somewhat larger (18% in the Portland region in December); most urban regions had maximum contributions in winter months and minima (∼5%–10%) in early summer months (Figure 5). The highest rural maximum EC contribution (10%) in the southwestern United States occurred in the Southern Arizona region in December, and many other rural regions had winter maximum contributions reflecting contributions from residential wood combustion (Figure 6). The maximum mean EC contribution in urban regions in the southwestern United States occurred in a region influenced by smoke (20% in the Northwest Nevada region in August). Minima for southwestern regions was around 4%–10% for urban regions and 1%–2% for rural regions. The urban Alaskan region had higher maximum EC mean contributions (14% in October) compared to the rural Alaska region (5% in July).

3.4.3. Seasonality

EC exhibited less seasonality than POM but followed similar spatial patterns. For example, in the eastern United States, the average seasonal ratio in rural EC was around 1.8, with the highest in the Boundary Waters region (2.6), similar to the largest seasonal ratio in POM. The urban seasonal ratio across eastern regions ranged from 1.4 to ∼3 (highest in the Dallas region), with an average of 1.9. EC had higher seasonality in the northwestern United States for both urban and rural regions, similar to POM. The highest northwestern rural seasonality occurred in the Northwest region (20.0) and Oregon/California region (19.0), in comparison to the 2005–2008 seasonality in these regions of 3.2 and 4.7, respectively. Less smoke-influenced regions, such as the rural Northern Great Plains, had a seasonal ratio of ∼3. EC seasonality in urban northwestern regions was much lower than rural regions, with an average seasonal ratio of 4.2, likely due to the additional winter urban sources. In the southwestern United States, the EC seasonality followed the spatial patterns in POM seasonality, with higher seasonal ratios in regions farther north that were influenced by smoke, such as the Great Basin region (13.0) and the urban Northwest Nevada region (12.2). Otherwise, average EC seasonality for rural and urban regions was 5.6 and 5.2, respectively. The lowest rural seasonality in the southwestern regions was in the (urban and rural) West Texas region (2.0), the urban Front Range Colorado region (3.0), and the Los Angeles region (3.1). Regions with winter maxima, such as the rural Southern Arizona and urban Phoenix/Tucson had seasonal ratios between 4 and 5, suggesting that the impacts of winter residential wood combustion on seasonality were less than the impacts of summer/fall biomass burning impacts observed at regions farther north.

3.5. Fine Dust

3.5.1. Absolute Concentration

In the eastern United States, long-range transport of north African dust (Prospero et al., 2021) influences FD concentrations during summer months in both rural and urban regions (Figures 2 and 3, respectively), such as the extreme "Godzilla" event in 2020 that influenced air quality and FD concentrations across the southeastern United States (Yu, Tan, et al., 2021). The maximum monthly mean rural FD was 2.6 µg m^{-3} in the Midsouth region in July and higher summer FD concentrations occurred in nearly all rural eastern regions, including the Southeast, Appalachia, Ohio River Valley, and East Coast regions (Figure 2). Temporal trends (2000–2021) in summer mean FD concentrations were flat and statistically insignificant for regions in the southeastern United States (Hand et al., 2024), suggesting summer mean FD concentrations have not significantly changed in this region over the past two decades; for example, in 2005–2008 the maximum mean FD concentration in the Midsouth region was 2.2 µg m^{-3}. Higher FD concentrations in the Virgin Islands region occurred from late May through early fall and reached a maximum of 4.4 µg m^{-3} in June. The influence of long-range FD transport was

also observed at urban regions, such as the maximum of 3.2 µg m^{-3} in the East Texas region in June, as well as the Midsouth, Dallas, East Texas/Gulf, Southeast, and Florida regions (Figure 3), although recall that CSN FD concentrations were biased low (−34%) relative to IMPROVE FD at collocated sites. The minimum rural mean FD concentrations in southeastern regions were lower than at urban regions (0.1–0.3 µg m^{-3} compared to 0.2–0.5 µg m^{-3}, respectively), suggesting additional urban sources.

In the northwestern United States, the rural Columbia River Gorge region had a maximum monthly mean FD concentration of 3.6 µg m^{-3} in August, compared to the 2005–2008 August maximum monthly mean of 1.9 µg m^{-3}; summer mean FD concentrations have increased in this area for unknown reasons (Hand et al., 2024). Most rural northwestern regions had maximum mean FD in July through September and urban maxima in June and September, except in Portland (April). Urban FD maxima were lower than rural maxima in northwestern regions, with a maximum mean FD of 1.2 µg m^{-3} in the urban Northwest region in September. Minimum mean concentrations were lower in rural regions of the northwestern United States (0.03–0.3 µg m^{-3}) compared to urban regions (0.2–0.4 µg m^{-3}).

The influence of FD on PM$_{2.5}$ mass in the southwestern United States is well known (Hand et al., 2017, 2024; Tong et al., 2012) and shown in Figures 6 and 7 for rural and urban regions, respectively. The maximum rural FD in the southwestern United States occurred in the West Texas region in June (3.1 µg m^{-3}), although many of the rural southern southwestern regions had maxima in spring months (e.g., Mogollon Plateau, Central Rockies, Southern Arizona, Colorado Plateau) when synoptic storms result in dust transport in the region (e.g., Rivera et al., 2009). Rural FD temporal trends in the southwestern region were statistically insignificant during all seasons, although earlier trend studies have identified increased FD in the southwestern U.S. depending on the years examined (Achakulwisut et al., 2017; Hand et al., 2016; Pu & Ginoux, 2018). In urban southwestern regions, the maximum FD mean concentration occurred in the Sacramento/Central Valley region (2.9 µg m^{-3}) in October, likely associated with agricultural activity (Rogge et al., 2007). All the urban California regions had maximum FD concentrations in October/November, whereas urban regions farther south had maximum in spring months (e.g., Northwest Nevada, Phoenix/Tucson, Albuquerque, and Las Vegas), likely influenced by spring dust transport. Like the rural West Texas region, the urban West Texas/El Paso region had a maximum FD concentration in June (2.9 µg m^{-3}). Minimum mean rural FD concentrations were higher than minima in other regions of the United States, generally greater than 0.2 µg m^{-3} and near 1 µg m^{-3} in the Southern Arizona and West Texas regions (Figure 6). Similarly, urban minima were higher (>0.4 µg m^{-3}), with the West Texas and Las Vegas regions having minimum mean FD concentrations greater than 1 µg m^{-3} (Figure 7).

3.5.2. Relative Concentration

FD contributions to RCFM were significant in regions of the eastern United States during summer months due to long-range transport of North African dust. For example, in the rural Midsouth and Southeast regions, FD contributed 30%–35% to RCFM in July. In other southeastern regions, the contributions were closer to 20% (Figure 2). In the Virgin Islands region, the maximum mean FD contribution was 57% in September, and greater than 40% from May to August. FD also contributed significantly to RCFM in urban eastern regions, with a maximum of 33% in the East Texas/Gulf region in July, 27% in the Dallas region in June, and 30% in the Florida region in June (Figure 3). In most rural northwestern regions, FD contributed a maximum of around 30% to RCFM and most regional maxima occurred during April, except for the Columbia River Gorge region (56%) in June (Figure 4). The maximum contribution of FD in urban northwestern regions occurred in the North Dakota region in June (22%) and the Northwestern region in April (19%) (Figure 5). Of all U.S. regions, the largest contributions of FD occurred in southwestern regions. The maximum rural mean contribution was 58% in the Great Basin region in April (Figure 6). Except for the maximum contributions in the rural California Coast (14%), Sierra Nevada (34%), and Southern California (33%) regions, all rural southwestern regions had contributions greater than 50% in spring months (Figure 6). Urban contributions to RCFM were lower than rural contributions (Figure 7), with the maximum monthly mean contribution in the urban West Texas region (43%) in April. Most urban regions had maxima around 20%–35%; however, urban California regions had much lower maximum contributions of around 10% (San Jose, Los Angeles, San Diego regions). Most of the maximum urban contributions occurred in April, suggesting that the regional transport of FD influences both urban and rural regions in the southwestern United States (Tong et al., 2023).

3.5.3. Seasonality

In the eastern United States, FD had the second highest seasonality of all the major species, less than AN but higher than POM due to the episodic impacts of long-range transport. In the East, the maximum rural seasonal ratio occurred in the Southeast region (11.4), compared to the lowest (2.6) in the Northeast region. The Midsouth also experienced a high degree of seasonality in monthly mean FD (8.7). Other rural regions had seasonal ratios around 4–5. The highest seasonal ratio in urban regions occurred in the Florida region (8.2), the East Texas/Gulf region (7.6), and the Midsouth region (6.5). Other urban regions had lower seasonal ratios of 2–3. Most of the rural northwestern regions had seasonal ratios around 11–12, except for the Northern Great Plains region (4.1). Urban FD seasonality was around 2–3, with a maximum of 7.0 in the North Dakota region. Similarly, urban FD seasonality in southwestern regions was considerably lower than rural regions, with ratios around 2–3, such as the maximum in the Albuquerque region (3.3). In contrast, the maximum rural seasonality was 14.4 in the Great Basin region, 8.8 in the Sierra Nevada region, and around 10 in the Colorado Plateau and Central Rockies regions. Regions farther south had lower seasonality (2–3), such as the Southern Arizona and West Texas regions, suggesting that these regions were influenced by FD year-round (Figure 6).

3.6. Sea Salt

3.6.1. Absolute Concentration

SS was noticeable mainly for coastal regions, such as in the eastern rural regions of the Northeast, East Coast, Southeast, and Virgin Islands regions (Figure 2). The maximum monthly mean rural SS concentration occurred at the Southeast and East Coast regions ($0.7 \ \mu g \ m^{-3}$), both in March. Similar urban maxima (0.7–$0.8 \ \mu g \ m^{-3}$) occurred in the Florida and East Texas/Gulf regions in late winter/early spring (Figure 3). The maximum monthly mean SS concentration at the rural Virgin Islands region was $2.1 \ \mu g \ m^{-3}$ in July. Maximum SS mean concentrations at northwestern regions was somewhat lower, with a rural maximum of $0.3 \ \mu g \ m^{-3}$ in the Oregon/California region and $0.5 \ \mu g \ m^{-3}$ in the urban Portland region, both in April (Figures 4 and 5, respectively). In the Alaska region, the rural maximum ($0.8 \ \mu g \ m^{-3}$) was somewhat larger than in the urban region ($0.6 \ \mu g \ m^{-3}$). Maximum mean SS concentrations were higher at coastal regions in the southwestern United States, such as the rural California Coast region ($1.9 \ \mu g \ m^{-3}$) and the urban San Jose region ($1.6 \ \mu g \ m^{-3}$), both in May (Figures 6 and 7, respectively). The rural Hawaii maximum mean SS concentration was $0.3 \ \mu g \ m^{-3}$, compared to $1.7 \ \mu g \ m^{-3}$ in the urban region, both in January. The difference in Hawaii maxima was due to the location of the rural and urban sites on different Hawaii islands, with rural sites further inland (Figures 6 and 7, respectively).

3.6.2. Relative Concentration

Contributions from SS to RCFM in eastern regions were apparent mainly at rural and urban coastal regions (Figures 2 and 3, respectively). In the East, the maximum mean contributions were around 15% for both urban and rural coastal regions; all other urban eastern regions had contributions less than 10%. Similar contributions occurred in the northwestern regions, with maximum mean contributions of 15% in the rural Northwest region in January and 11% in the urban Puget Sound region in April (Figures 4 and 5, respectively). In the southwestern regions, the greatest maximum contributions also occurred at coastal regions, such as the rural California Coast (39%) and the urban San Jose region (25%), both in May (Figures 6 and 7, respectively). The highest monthly mean SS contribution in urban regions occurred at the Hawaii region (43%) in January, and the rural Virgin Island region in January (47%), and the rural Alaska region in December (48%).

3.6.3. Seasonality

The highest degree of seasonality in SS for regions in the East occurred at the rural Boundary Waters region (10.0), where mean concentrations were low most of the year ($<0.1 \ \mu g \ m^{-3}$) but increased during winter months (Figure 2), perhaps due to road salt applications (McNamara et al., 2020). The urban maximum seasonal ratio occurred in the Chicago region (6.7) and the Michigan/Great Lakes region (5.5). Most other rural and urban regions had seasonal ratios around 2–4. These ratios were similar to those in the rural northwestern regions, with the highest in the rural and urban Northwest regions (4.5 and 6.3, respectively) and the urban North Dakota region (6.9). In the southwestern regions, the largest seasonal ratio occurred in the Mogollon Plateau region (7.7) and the urban Utah (7.6) and Las Vegas (7.3) regions. Most other rural and urban regions had seasonal ratios around 4–5. The regions along the coast had seasonal ratios around 4 (rural California Coast) and 3 (urban San Jose).
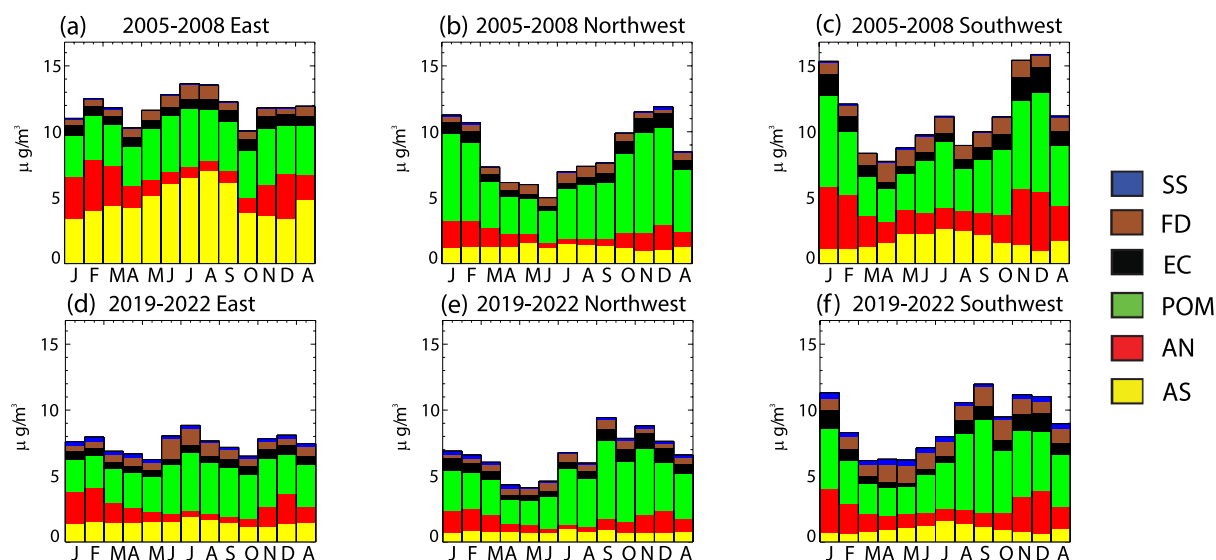
Figure 9. Urban CSN area, monthly average monthly mean speciated PM$_{2.5}$ mass concentrations (µg m^{-3}) for 2005–2008 for the (a) East, (b) Northwest, Southwest and 2019–2022 for the (d) East, (e) Northwest, and (f) Southwest for ammonium sulfate (AS), ammonium nitrate (AN), particulate organic matter (POM), elemental carbon (EC), fine dust (FD), and sea salt (SS).

4. Summary and Conclusions

The variability observed in the spatial and seasonal patterns in 2019–2022 monthly mean aerosol species concentrations for the rural/remote regions of the IMPROVE network and the urban/suburban regions in the CSN were indicative of the spatial extent of aerosol sources, atmospheric processes, and regional transport. This study updates earlier analyses (Hand, Schichtel, & Pitchford et al., 2012; Malm et al., 2004) and is an opportunity to compare the spatial and seasonal variability of PM over the past two decades in the context of changing sources. Summaries of regional monthly mean concentrations for the three main areas presented here (i.e., eastern, northwestern, and southwestern United States) are shown for 2005–2008 (Hand, Schichtel, & Pitchford et al., 2012) and 2019–2022 for IMPROVE (Figure 8) and CSN (Figure 9). Similar figures for rural and urban mass fraction are included as Figure S1 and S2 in Supporting Information S1, respectively, as are summaries of seasonal variability (Figure S3 and Figure S4 in Supporting Information S1, respectively). Results presented in Figures 8 and 9 correspond to averages over all the regions available within an area for each period. Caveats regarding comparisons over the two periods include the different OM/OC ratios that were applied to both IMPROVE and CSN data. OC data from both networks in 2005–2008 were converted to POM using a constant OM/OC value of 1.8 (Hand, Schichtel, & Pitchford et al., 2012), while in 2019–2022 monthly varying OM/OC values were applied to IMPROVE OC data and warm/cool month OM/OC values were applied to CSN OC data. IMPROVE FD was increased by 15% in the dust algorithm for the 2019–2022 period, while CSN FD data were not adjusted. Chloride ion data instead of chlorine XRF data were used to calculate SS for CSN in 2019–2022. Importantly, changes in CSN laboratory contractors and analyses occurred in 2015–2018 that could significantly influence trends in CSN ion, carbon, and XRF data. While comparisons of large-scale seasonal and spatial patterns for the two periods are still relevant, evaluating trends in CSN data is problematic if the data are not adjusted during these shifts (Kaur et al., 2024). Finally, while most regions are the same between periods, some sites within regions may differ due to site closures or new sites coming online.

AS and its contribution to PM have decreased dramatically between 2005–2008 and 2019–2022 due to reductions in precursor emissions. The average annual mean AS contributions to RCFM are now ~20% or less, with the highest contributions in the East. In 2005–2008, AS contributions were often greater than 50% in the East (Figures 8a, 8d, 9a and 9d). In both periods, AS concentrations were similar in rural and urban areas (Figures 8 and 9, respectively), suggesting regional impacts due to secondary formation processes. In 2019–2022, annual mean urban and rural AS concentrations were around 1.0–2.0 µg m^{-3} in the eastern area, larger than in the northwestern (0.5–0.8 µg m^{-3}) and southwestern areas (0.7–1.0 µg m^{-3}) due to higher emissions in the East.

Previously, both rural and urban AS peaked in summer in the East (see Figures 8a and 9a, respectively), but stronger reductions in summer mean AS concentrations relative to other seasons has led to a flattening of AS seasonality, with low or nonexistent summer peaks (Figures 8d and 9d for rural and urban areas, respectively). In 2019–2022, the eastern urban and rural average seasonal ratios were near 2, compared to previous (2005–2008) average estimates near 3 (Hand, Schichtel, & Pitchford et al., 2012). Unlike in eastern regions, AS peaked in summer in many southwestern rural and urban regions (Figures 8f and 9f, respectively), and that seasonality has not changed considerably since 2005–2008 (see Figures S3 and S4 in Supporting Information S1), in part because of similar seasonal temporal trends in AS in those regions (Hand et al., 2024).

Annual mean AN decreased between both periods for all rural and urban regions (Figures 8 and 9, respectively), but with the lowest reduction in the northwestern region. This spatial pattern is consistent with the trend analysis by Hand et al. (2024) that observed relatively weaker AN trends in the northwestern United States compared to the rest of the country. Annual mean urban concentrations were higher than the rural concentrations across the United States in both periods. In 2019–2022, the average eastern urban annual mean AN concentration was twice the rural average value (1.2 µg m^{-3} vs. 0.6 µg m^{-3}, respectively), almost three times higher in the northwestern U.S. regions (1.0 µg m^{-3} vs. 0.4 µg m^{-3}, respectively) and over four times higher (1.7 µg m^{-3} vs. 0.4 µg m^{-3}, respectively) in the southwestern U.S. regions. Regions with proximity to agricultural activity in the Midwest had higher urban and rural mean concentrations, as well as regions near areas with oil and gas activity and biomass smoke impacts. High annual mean AN concentrations occurred in large urban areas, especially in California regions, although these concentrations have decreased over the past two decades. For example, the annual mean urban AN concentration in the Southwest area decreased by 60%, from 2.7 µg m^{-3} in 2005–2008 to 1.7 µg m^{-3} in 2019–2022 (Figures 9c and 9f, respectively), reflecting reductions in NO$_x$ emissions (Yu, McDonald, & Harley, 2021).

AN annual mean contribution to RCFM was around ∼10%–20% for urban and rural regions in both periods and could reach up to ∼30% during winter months. Due to favorable formation conditions in winter, AN in nearly all regions had strong winter maxima and low summer minima (see Figures 8 and 9, Figures S3 and S4 in Supporting Information S1), except for regions influenced by biomass smoke. In nearly all urban and rural regions, except the rural southwestern United States (∼3), the maximum mean concentration (typically in winter) was 6–8 times higher than the minimum concentration in 2019–2022, consistent with seasonal ratios from 2005 to 2008.

POM is now the major contributor to RCFM in all continental U.S. regions, with an average annual mean contribution over 40% in rural and urban regions (Figures 8 and 9, respectively). The highest rural and urban annual mean contributions occurred in the northwestern United States (59% and 52%, respectively). These high contributions were due to the influence of biomass burning which led to high summer concentrations, especially for rural regions. Peaks in rural POM in summer occurred in both periods (Figures 8b and 8e, respectively) but the impact of high fire years during 2019–2022 was evident in Figures 8e and 8f; Figures 9e and 9f for rural and urban areas, respectively. Average annual mean POM concentrations were highest of all the species, with larger urban concentrations. Rural average annual mean POM concentrations ranged from ∼1.5 to 2.5 µg m^{-3}, with largest values in the northwestern area, while urban annual mean concentrations ranged from ∼3 to 4 µg m^{-3}, with the largest values in the southwestern area.

High summer POM concentrations also led to large seasonal variability in POM. In the rural northwestern and southwestern regions, the average seasonal ratio was over 20 and 10, respectively, compared to an average of 3.6 in eastern regions. The average seasonal variability in urban regions was significantly lower (5.1, 4.0, and 2.3 in northwestern, southwestern, and eastern regions) due to additional urban sources in winter (Figure 9). In fact, the strong urban winter maxima in the northwestern and southwestern areas in 2005–2008 shifted to summer-fall maxima in 2019–2022 (Figure 9) due to the impacts from fires.

Urban EC concentrations were higher than rural EC concentrations across the United States, although recall that CSN EC was biased high (28%) relative to IMPROVE EC based on collocated data. Average annual mean concentrations for all urban areas were around 0.6–0.9 µg m^{-3} compared to ∼0.2 µg m^{-3} for rural regions. Rural EC spatial and seasonal patterns followed those of POM in regions influenced by biomass smoke (Figure 8 and Figure S3 in Supporting Information S1). Urban winter maxima, especially in western regions during both periods, reflected additional urban sources such as residential wood combustion (Figure 9 and Figure S4 in Supporting Information S1). The seasonal ratio in EC was lower for urban relative to rural regions because of these additional sources, but the impacts from biomass burning in 2019–2022 were still evident, especially in western

urban regions (1.9, 4.2, and 5.2 for eastern, northwestern, and southwestern areas, respectively). This smoke influence had a stronger impact on rural seasonality (11.7 in the northwestern area, compared to 1.8 and 5.6 in the eastern and southwestern areas, respectively). EC contributions to RCFM were relatively low, around 5% and 10% for all rural and urban regions, respectively, and they have stayed consistent since 2005–2008 (Figures S1 and S2 in Supporting Information S1).

Urban and rural FD concentrations were influenced by local, regional, and long-range transport. When comparing urban and rural regional mean FD concentrations, recall that CSN FD was biased low relative to IMPROVE FD for both periods and that IMPROVE FD data were increased by 15% relative to the IMPROVE values reported in 2005–2008 by Hand, Schichtel, & Pitchford et al. (2012). In the eastern United States in summer, North African dust transport influenced both rural and urban FD concentrations during both periods (Figures 8 and 9, respectively). FD concentrations were also higher near agricultural areas for both urban and rural regions, such as the Central Great Plains/Central U.S. and Northern Great Plains, and the spring dust phenomenon influenced FD in both rural and urban regions in the southwestern United States during both periods. In 2019–2022, average annual mean urban and rural FD concentrations in the eastern and northwestern regions were around 0.5–0.7 µg m^{-3}, and greater than 1.0 µg m^{-3} in the urban and rural southwestern regions. Annual mean contributions of FD to RCFM were around 10% for both urban and rural regions in the East, but rural contributions were double urban contributions in the northwestern regions (14% vs. 7%, respectively) and southwestern regions (28% vs. 14%, respectively).

The impacts of episodic dust events led to large seasonal variability in FD concentrations, especially in rural regions (Figure S3 in Supporting Information S1). The average rural FD seasonal ratio was highest in the northwestern area (10.6) relative to the southwestern (7.2) and eastern areas (5.8). The seasonal ratio in the 2005–2008 rural northwestern region was lower (7.8), suggesting that perhaps stronger or more frequent impacts may now by influencing rural FD in northwestern regions. In fact, Hand et al. (2024) reported that FD has increased over the past two decades only in summer for some sites in the rural northwestern United States, such as in the Columbia River Gorge region. In contrast, urban FD seasonality was relatively low (4.1, 3.7, and 2.9 for the eastern, northwestern, and southwestern areas, respectively) and has stayed consistent over time (Figure S4 in Supporting Information S1). Although episodic events appeared to influence monthly mean FD concentrations in urban regions, additional urban sources of FD may be contributing to a lower seasonal variability.

Except in coastal regions, SS concentrations and contributions to RCFM were negligible in most urban and rural regions. The impacts of using chloride ion in 2019–2022 instead of chlorine to calculate SS for CSN data can be seen in comparing the two time periods in Figure 9. Average annual mean SS concentrations were less than 0.2 µg m^{-3} in all areas, except for the urban southwestern areas (0.3 µg m^{-3}). Average annual mean urban SS concentrations in 2019–2022 were typically double rural concentrations, perhaps due to the application of road salt (McNamara et al., 2020), and average annual mean rural and urban SS contributions to RCFM were around 3% in all areas (Figures S1 and S2 in Supporting Information S1, respectively). The seasonal ratio in SS was similar in urban and rural regions, with an average seasonal ratio around 3–4 across the United States.

These results have demonstrated the importance of integrating long-term ground-based monitoring to understand the composition and seasonality of major aerosol species across the United States. Comparisons to previous studies has demonstrated that the magnitude, contribution, and seasonality of speciated PM$_{2.5}$ has shifted over the past decades, leading to organic aerosol dominating PM$_{2.5}$ mass in urban and rural regions across the United States. These changes are largely due to changing emissions, as reductions in precursor emissions have led to decreased sulfate, nitrate, and some carbonaceous aerosols. However, the role of biomass smoke has grown in importance, at least during the period investigated in this study. Differences in urban and rural aerosol spatial and seasonal patterns also indicated the importance of local urban sources to PM$_{2.5}$. Evaluating the urban and rural monthly variability of major aerosol species is necessary for designing mitigation strategies to reduce PM$_{2.5}$ in the atmosphere (Li et al., 2024) and these results suggest that novel approaches will be necessary to reduce unregulated anthropogenic sources and natural sources, such as biomass smoke and dust, which are predicted to increase with a changing climate (e.g., Abatzoglou & Williams, 2016; Achakulwisut et al., 2019).

Conflict of Interest

The authors declare no conflicts of interest relevant to this study.

Data Availability Statement

The IMPROVE and CSN data sets (Federal Land Manager Environmental Database, 2024) are accessible from its reference and publicly available (https://views.cira.colostate.edu/fed/QueryWizard/).

References

Abatzoglou, J. T., & Williams, A. P. (2016). Impact of anthropogenic climate change on wildfire across western US forests. *Proceedings of the National Academy of Sciences*, *113*(42), 11770–11775. https://doi.org/10.1029/2018GL080959

Achakulwisut, P., Anenberg, S. C., Neumann, J. E., Penn, S. L., Weiss, N., Crimmins, A., et al. (2019). Effects of increasing aridity on ambient dust and public health in the US Southwest under climate change. *GeoHealth*, *3*(5), 127–144. https://doi.org/10.1029/2019GH000187

Achakulwisut, P., Shen, L., & Mickley, L. J. (2017). What controls springtime fine dust variability in the western United States? Investigating the 2002–2015 increase in fine dust in the US southwest. *Journal of Geophysical Research: Atmospheres*, *122*(22), 12449–412467. https://doi.org/10.1002/2017JD027208

Aiken, A. C., Decarlo, P. F., Kroll, J. H., Worsnop, D. R., Huffman, J. A., Docherty, K. S., et al. (2008). O/C and OM/OC ratios of primary, secondary, and ambient organic aerosols with high-resolution time-of-flight aerosol mass spectrometry. *Environmental Science and Technology*, *42*(12), 4478–4485. https://doi.org/10.1021/es703009q

Aldhaif, A. M., Lopez, D. H., Dadashazar, H., & Sorooshian, A. (2020). Sources, frequency, and chemical nature of dust events impacting the United States East Coast. *Atmospheric Environment*, *231*, 12. https://doi.org/10.1016/j.atmosenv.2020.117456

Allen, H. M., Draper, D. C., Ayres, B. R., Ault, A., Bondy, A., Takahama, S., et al. (2015). Influence of crustal dust and sea spray supermicron particle concentrations and acidity on inorganic NO3- aerosol during the 2013 Southern Oxidant and Aerosol Study. *Atmospheric Chemistry and Physics*, *15*(18), 10669–10685. https://doi.org/10.5194/acp-15-10669-2015

Attwood, A., Washenfelder, R., Brock, C., Hu, W., Baumann, K., Campuzano-Jost, P., et al. (2014). Trends in sulfate and organic aerosol mass in the Southeast US: Impact on aerosol optical depth and radiative forcing. *Geophysical Research Letters*, *41*(21), 7701–7709. https://doi.org/10.1002/2014GL061669

Ault, A. P., Gaston, C. J., Wang, Y., Dominguez, G., Thiemens, M. H., & Prather, K. A. (2010). Characterization of the single particle mixing state of individual ship plume events measured at the port of Los Angeles. *Environmental Science and Technology*, *44*(6), 1954–1961. https://doi.org/10.1021/es902985h

Bae, M.-S., Demerjian, K. L., & Schwab, J. J. (2006). Seasonal estimation of organic mass to organic carbon in PM2. 5 at rural and urban locations in New York state. *Atmospheric Environment*, *40*(39), 7467–7479. https://doi.org/10.1016/j.atmosenv.2006.07.008

Beachley, G., Phuchalski, M., Rogers, C., & Lear, G. (2016). A summary of long-term trends in sulfur and nitrogen deposition in the United States 1990–2013. *JSM Environmental Science & Ecology*, *4*(2), 1030. https://doi.org/10.47739/2333-7141/1030

Benedict, K. B., Prenni, A. J., Carrico, C. M., Sullivan, A. P., Schichtel, B. A., & Collett, J. L. (2017). Enhanced concentrations of reactive nitrogen species in wildfire smoke. *Atmospheric Environment*, *148*, 8–15. https://doi.org/10.1016/j.atmosenv.2016.10.030

Benish, S. E., Bash, J. O., Foley, K. M., Appel, K. W., Hogrefe, C., Gilliam, R., & Pouliot, G. (2022). Long-term regional trends of nitrogen and sulfur deposition in the United States from 2002 to 2017. *Atmospheric Chemistry and Physics*, *22*(19), 12749–12767. https://doi.org/10.5194/acp-22-12749-2022

Blanchard, C., Hidy, G., Shaw, S., Baumann, K., & Edgerton, E. (2016). Effects of emission reductions on organic aerosol in the southeastern United States. *Atmospheric Chemistry and Physics*, *16*(1), 215–238. https://doi.org/10.5194/acp-16-215-2016

Blanchard, C., Hidy, G., Tanenbaum, S., Edgerton, E., & Hartsell, B. (2013). The Southeastern Aerosol Research and Characterization (SEARCH) study: Temporal trends in gas and PM concentrations and composition, 1999–2010. *Journal of the Air and Waste Management Association*, *63*(3), 247–259. https://doi.org/10.1080/10962247.2012.748523

Bond, T. C., Doherty, S. J., Fahey, D. W., Forster, P. M., Berntsen, T., DeAngelo, B. J., et al. (2013). Bounding the role of black carbon in the climate system: A scientific assessment. *Journal of Geophysical Research: Atmospheres*, *118*(11), 5380–5552. https://doi.org/10.1002/jgrd.50171

Bozlaker, A., Prospero, J. M., Price, J., & Chellam, S. (2019). Identifying and quantifying the impacts of advected North African dust on the concentration and composition of airborne fine particulate matter in Houston and Galveston, Texas. *Journal of Geophysical Research: Atmospheres*, *124*(22), 12282–12300. https://doi.org/10.1029/2019JD030792

Brown, S. G., Lee, T., Roberts, P. T., & Collett, J. L. (2016). Wintertime residential biomass burning in Las Vegas, Nevada; marker components and apportionment methods. *Atmosphere*, *7*(4), 58. https://doi.org/10.3390/atmos7040058

Busby, B. D., Ward, T. J., Turner, J. R., & Palmer, C. P. (2016). Comparison and evaluation of methods to apportion ambient PM2. 5 to residential wood heating in Fairbanks, AK. *Aerosol and Air Quality Research*, *16*(3), 492–503. https://doi.org/10.4209/aaqr.2015.04.0235

Chan, E. A. W., Gantt, B., & McDow, S. (2018). The reduction of summer sulfate and switch from summertime to wintertime PM2.5 concentration maxima in the United States. *Atmospheric Environment*, *175*, 25–32. https://doi.org/10.1016/j.atmosenv.2017.11.055

Chen, Y., Shen, H., & Russell, A. G. (2019). Current and future responses of aerosol ph and composition in the US to declining SO2 emissions and increasing NH3 emissions. *Environmental Science and Technology*, *53*(16), 9646–9655. https://doi.org/10.1021/acs.est.9b02005

Cheng, B., Alapaty, K., & Arunachalam, S. (2024). Spatiotemporal trends in PM2. 5 chemical composition in the conterminous US during 2006–2020. *Atmospheric Environment*, *316*, 120188. https://doi.org/10.1016/j.atmosenv.2023.120188

Childs, M. L., Li, J., Wen, J., Heft-Neal, S., Driscoll, A., Wang, S., et al. (2022). Daily local-level estimates of ambient wildfire smoke PM2. 5 for the contiguous US. *Environmental Science and Technology*, *56*(19), 13607–13621. https://doi.org/10.1021/acs.est.2c02934

Chow, J. C., Lowenthal, D. H., Chen, L.-W. A., Wang, X., & Watson, J. G. (2015). Mass reconstruction methods for PM2. 5: A review. *Air Quality, Atmosphere & Health*, *8*(3), 243–263. https://doi.org/10.1007/s11869-015-0338-3

Chow, J. C., Wang, X., Sumlin, B. J., Gronstal, S. B., Chen, L.-W. A., Trimble, D. L., et al. (2015). Optical calibration and equivalence of a multiwavelength thermal/optical carbon analyzer. *Aerosol and Air Quality Research*, *15*(4), 1145–1159. https://doi.org/10.4209/aaqr.2015.02.0106

Chow, J. C., Watson, J. G., Chen, L.-W. A., Chang, M. O., Robinson, N. F., Trimble, D., & Kohl, S. (2007). The IMPROVE_A temperature protocol for thermal/optical carbon analysis: Maintaining consistency with a long-term database. *Journal of the Air and Waste Management Association*, *57*(9), 1014–1023. https://doi.org/10.3155/1047-3289.57.9.1014

Creamean, J. M., Spackman, J. R., Davis, S. M., & White, A. B. (2014). Climatology of long-range transported Asian dust along the West Coast of the United States. *Journal of Geophysical Research: Atmospheres*, *119*(21), 12171–112185. https://doi.org/10.1002/2014JD021694

Dillner, A. M., Phuah, C. H., & Turner, J. R. (2009). Effects of post-sampling conditions on ambient carbon aerosol filter measurements. *Atmospheric Environment*, *43*(37), 5937–5943. https://doi.org/10.1016/j.atmosenv.2009.08.009

Dong, C., Williams, A. P., Abatzoglou, J. T., Lin, K., Okin, G. S., Gillespie, T. W., et al. (2022). The season for large fires in Southern California is projected to lengthen in a changing climate. *Communications Earth & Environment*, *3*(1), 22. https://doi.org/10.1038/s43247-022-00344-6

Du, E., de Vries, W., Galloway, J. N., Hu, X., & Fang, J. (2014). Changes in wet nitrogen deposition in the United States between 1985 and 2012. *Environmental Research Letters*, *9*, 095004. https://doi.org/10.1088/1748-9362/9/9/095004

Ellis, R., Jacob, D. J., Sulprizio, M. P., Zhang, L., Holmes, C., Schichtel, B., et al. (2013). Present and future nitrogen deposition to national parks in the United States: Critical load exceedances. *Atmospheric Chemistry and Physics*, *13*(17), 9083–9095. https://doi.org/10.5194/acp-13-9038-2013

El-Zanan, H. S., Lowenthal, D. H., Zielinska, B., Chow, J. C., & Kumar, N. (2005). Determination of the organic aerosol mass to organic carbon ratio in IMPROVE samples. *Chemosphere*, *60*(4), 485–496. https://doi.org/10.1016/j.chemosphere.2005.01.005

El-Zanan, H. S., Zielinska, B., Mazzoleni, L. R., & Hansen, D. A. (2009). Analytical determination of the aerosol organic mass-to-organic carbon ratio. *Journal of the Air and Waste Management Association*, *59*(1), 58–69. https://doi.org/10.3155/1047-3289.59.1.58

EPA, U. S. (2003). Guidance for tracking progress under the regional haze Rule, EPA-454/B-03-004.

EPA, U. S. (2004). PM2.5 speciation network newsletter. Retrieved from https://www3.epa.gov/ttnamti1/files/ambient/pm25/spec/spnews1.pdf

EPA, U. S. (2018). Technical guidance on tracking visibility progress for the second implementation period of the Regional Haze program, EPA-454/R-18-010.

Federal Land Manager Environmental Database. (2024). IMPROVE aerosol composition dataset, 1988 to 2024 [Dataset]. *CSN aerosol composition dataset*. https://views.cira.colostate.edu/fed/QueryWizard/

Feng, J., Chan, E., & Vet, R. (2020). Air quality in the eastern United States and eastern Canada for 1990–2015: 25 years of change in response to emission reductions of SO2 and NOx in the region. *Atmospheric Chemistry and Physics*, *20*(5), 3107–3134. https://doi.org/10.5194/acp-20-3107-2020

Frank, N. H. (2006). Retained nitrate, hydrated sulfates, and carbonaceous mass in federal reference method fine particulate matter for six eastern US cities. *Journal of the Air and Waste Management Association*, *56*(4), 500–511. https://doi.org/10.1080/10473289.2006.10464517

Gebhart, K. A., Day, D. E., Prenni, A. J., Schichtel, B. A., Hand, J. L., & Evanoski-Cole, A. R. (2018). Visibility impacts at Class I areas near the Bakken oil and gas development. *Journal of the Air and Waste Management Association*, *68*(5), 477–493. https://doi.org/10.1080/10962247.2018.1429334

Ginoux, P., Prospero, J. M., Gill, T. E., Hsu, N. C., & Zhao, M. (2012). Global-scale attribution of anthropogenic and natural dust sources and their emission rates based on MODIS Deep Blue aerosol products. *Reviews of Geophysics*, *50*(3). https://doi.org/10.1029/2012RG000388

Gorham, K. A., Raffuse, S. M., Hyslop, N. P., & White, W. H. (2021). Comparison of recent speciated PM2. 5 data from collocated CSN and IMPROVE measurements. *Atmospheric Environment*, *244*, 117977. https://doi.org/10.1016/j.atmosenv.2020.117977

Hallar, A. G., Lowenthal, D. H., Clegg, S. L., Samburova, V., Taylor, N., Mazzoleni, L. R., et al. (2013). Chemical and hygroscopic properties of aerosol organics at Storm Peak Laboratory. *Journal of Geophysical Research: Atmospheres*, *118*(10), 4767–4779. https://doi.org/10.1002/jgrd.50373

Hand, J., Kreidenweis, S., Sherman, D. E., Collett Jr, J., Hering, S., Day, D., & Malm, W. (2002). Aerosol size distributions and visibility estimates during the Big Bend regional aerosol and visibility observational (BRAVO) study. *Atmospheric Environment*, *36*(32), 5043–5055. https://doi.org/10.1016/S1352-2310(02)00568-X

Hand, J., Schichtel, B., Malm, W., & Frank, N. (2013). Spatial and temporal trends in PM2. 5 organic and elemental carbon across the United States. *Advances in Meteorology*, *2013*(1), 367674. https://doi.org/10.1155/2013/367674

Hand, J. L., Copeland, S. A., Chow., J., Dillner, A. M., Hyslop, N. P., Malm, W. C., et al. (2023). *IMPROVE (interagency monitoring of protected visual environments): Spatial and seasonal patterns and temporal variability of haze and its constituents in the United States: Report VI, cooperative Institute for research in the atmosphere*. Colorado State University. https://doi.org/10.25675/10217/237177

Hand, J. L., Gebhart, K. A., Schichtel, B. A., & Malm, W. C. (2012c). Increasing trends in wintertime particulate sulfate and nitrate ion concentrations in the Great Plains of the United States (2000-2010). *Atmospheric Environment*, *55*, 107–110. https://doi.org/10.1016/j.atmosenv.2012.03.050

Hand, J. L., Gill, T., & Schichtel, B. (2017). Spatial and seasonal variability in fine mineral dust and coarse aerosol mass at remote sites across the United States. *Journal of Geophysical Research: Atmospheres*, *122*(5), 3080–3097. https://doi.org/10.1002/2016JD026290

Hand, J. L., Prenni, A. J., Copeland, S., Schichtel, B. A., & Malm, W. C. (2020). Thirty years of the clean air act amendments: Impacts on haze in remote regions of the United States (1990–2018). *Atmospheric Environment*, *243*, 117865. https://doi.org/10.1016/j.atmosenv.2020.117865

Hand, J. L., Prenni, A. J., & Schichtel, B. A. (2024). Trends in seasonal mean speciated aerosol composition in remote areas of the United States from 2000 through 2021. *Journal of Geophysical Research: Atmospheres*, *129*(2), e2023JD039902. https://doi.org/10.1029/2023JD039902

Hand, J. L., Prenni, A. J., Schichtel, B. A., Malm, W. C., & Chow, J. C. (2019). Trends in remote PM2.5 residual mass across the United States: Implications for aerosol mass reconstruction in the IMPROVE network. *Atmospheric Environment*, *203*, 141–152. https://doi.org/10.1016/j.atmosenv.2019.01.049

Hand, J. L., Schichtel, B., Malm, W., Pitchford, M., & Frank, N. (2014). Spatial and seasonal patterns in urban influence on regional concentrations of speciated aerosols across the United States. *Journal of Geophysical Research: Atmospheres*, *119*(22), 12832–812849. https://doi.org/10.1002/2014JD022328

Hand, J. L., Schichtel, B. A., Malm, W. C., & Pitchford, M. L. (2012b). Particulate sulfate ion concentration and SO2 emission trends in the United States from the early 1990s through 2010. *Atmospheric Chemistry and Physics*, *12*(21), 10353–10365. https://doi.org/10.5194/acp-12-10353-2012

Hand, J. L., Schichtel, B. A., Pitchford, M., Malm, W. C., & Frank, N. H. (2012a). Seasonal composition of remote and urban fine particulate matter in the United States. *Journal of Geophysical Research*, *117*(D5), D05209. https://doi.org/10.1029/2011jd017122

Hand, J. L., White, W., Gebhart, K., Hyslop, N., Gill, T., & Schichtel, B. (2016). Earlier onset of the spring fine dust season in the southwestern United States. *Geophysical Research Letters*, *43*(8), 4001–4009. https://doi.org/10.1002/2016GL068519

Heald, C., Collett, J. L., Jr., Lee, T., Benedict, K. B., Schwandner, F. M., Li, Y., et al. (2012). Atmospheric ammonia and particulate inorganic nitrogen over the United States. *Atmospheric Chemistry and Physics*, *12*(21), 10295–10312. https://doi.org/10.5194/acp-12-10295-2012

Heald, C. L., & Kroll, J. (2020). The fuel of atmospheric chemistry: Toward a complete description of reactive organic carbon. *Science Advances*, *6*(6), eaay8967. https://doi.org/10.1126/sciadv.aay8967

Hersey, S. P., Craven, J. S., Metcalf, A. R., Lin, J., Lathem, T., Suski, K. J., et al. (2013). Composition and hygroscopicity of the Los Angeles aerosol: CalNex. *Journal of Geophysical Research: Atmospheres*, *118*(7), 3016–3036. https://doi.org/10.1002/jgrd.50307

Hidy, G., Blanchard, C., Baumann, K., Edgerton, E., Tanenbaum, S., Shaw, S., et al. (2014). Chemical climatology of the southeastern United States, 1999–2013. *Atmospheric Chemistry and Physics*, *14*(21), 11893–11914. https://doi.org/10.5194/acp-14-11893-2014

Hu, C., Griffis, T. J., Baker, J. M., Wood, J. D., Millet, D. B., Yu, Z., & Lee, X. (2020). Modeling the sources and transport processes during extreme ammonia episodes in the US Corn Belt. *Journal of Geophysical Research: Atmospheres*, *125*(2), e2019JD031207. https://doi.org/10.1029/2019JD031207

Husar, R. B., Tratt, D., Schichtel, B. A., Falke, S., Li, F., Jaffe, D., et al. (2001). Asian dust events of April 1998. *Journal of Geophysical Research*, *106*(D16), 18317–18330. https://doi.org/10.1029/2000JD900788

Jimenez, J. L., Canagaratna, M., Donahue, N., Prevot, A., Zhang, Q., Kroll, J. H., et al. (2009). Evolution of organic aerosols in the atmosphere. *Science*, *326*(5959), 1525–1529. https://doi.org/10.1126/science.1180353

Kaur, K., Krall, J. R., Ivey, C., Holmes, H. A., & Kelly, K. E. (2024). Impact of Chemical Speciation Network method changes on time series ion and carbon species concentrations. *Aerosol Science and Technology*, *58*(11), 1–15. https://doi.org/10.1080/02786826.2024.2384921

Kim, D., Chin, M., Cruz, C. A., Tong, D., & Yu, H. (2021). Spring dust in western north America and its interannual variability—Understanding the role of local and transported dust. *Journal of Geophysical Research: Atmospheres*, *126*(22), e2021JD035383. https://doi.org/10.1029/2021JD035383

Kim, E., & Hopke, P. K. (2004). Comparison between conditional probability function and nonparametric regression for fine particle source directions. *Atmospheric Environment*, *38*(28), 4667–4673. https://doi.org/10.1016/j.atmosenv.2004.05.035

Kim, P. S., Jacob, D. J., Fisher, J. A., Travis, K., Yu, K., Zhu, L., et al. (2015). Sources, seasonality, and trends of Southeast US aerosol: An integrated analysis of surface, aircraft, and satellite observations with the GEOS-Chem chemical transport model. *Atmospheric Chemistry and Physics*, *15*(18), 10411–10433. https://doi.org/10.5194/acp-15-10411-2015

Lambert, A., Hallar, A. G., Garcia, M., Strong, C., Andrews, E., & Hand, J. L. (2020). Dust impacts of rapid agricultural expansion on the Great Plains. *Geophysical Research Letters*, *47*(20), e2020GL090347. https://doi.org/10.1029/2020GL090347

Lawal, A. S., Guan, X., Liu, C., Henneman, L. R., Vasilakos, P., Bhogineni, V., et al. (2018). Linked response of aerosol acidity and ammonia to SO2 and NOx emissions reductions in the United States. *Environmental Science and Technology*, *52*(17), 9861–9873. https://doi.org/10.1021/acs.est.8b00711

Lee, T., Yu, X.-Y., Ayres, B., Kreidenweis, S. M., Malm, W. C., & Collett Jr, J. L. (2008). Observations of fine and coarse particle nitrate at several rural locations in the United States. *Atmospheric Environment*, *42*(11), 2720–2732. https://doi.org/10.1016/j.atmosenv.2007.05.016

Lehmann, C. M., & Gay, D. A. (2011). Monitoring long-term trends of acidic wet deposition in US precipitation: Results from the National Atmospheric Deposition Program. *PowerPlant Chemistry*, *13*(7), 378–385.

Li, C., Martin, R. V., & Donkelaar, V. (2024). Understanding reductions of PM$_{2.5}$ concentration and its chemical composition in the United States: Implications for mitigation strategies. *Environmental Science and Technology Air*, *1*(7), 637–645. https://doi.org/10.1021/acsestair.4c00004

Lindaas, J., Pollack, I. B., Garofalo, L. A., Pothier, M. A., Farmer, D. K., Kreidenweis, S. M., et al. (2021). Emissions of reactive nitrogen from western U.S. Wildfires during summer 2018. *Journal of Geophysical Research: Atmospheres*, *126*(2), e2020JD032657. https://doi.org/10.1029/2020JD032657

Lowenthal, D., & Kumar, N. (2006). Light scattering from sea-salt aerosols at interagency monitoring of protected visual environments (IMPROVE) sites. *Journal of the Air and Waste Management Association*, *56*(5), 636–642. https://doi.org/10.1080/10473289.2006.10464478

Lowenthal, D., Zielinska, B., Mason, B., Samy, S., Samburova, V., Collins, D., et al. (2009). Aerosol characterization studies at great smoky mountains national Park, summer 2006. *Journal of Geophysical Research*, *114*(D8). https://doi.org/10.1029/2008JD011274

Lowenthal, D., Zielinska, B., Samburova, V., Collins, D., Taylor, N., & Kumar, N. (2015). Evaluation of assumptions for estimating chemical light extinction at US national parks. *Journal of the Air and Waste Management Association*, *65*(3), 249–260. https://doi.org/10.1080/10962247.2014.986307

Malm, W., Schichtel, B., Hand, J., & Prenni, A. (2020). Implications of organic mass to carbon ratios increasing over time in the rural United States. *Journal of Geophysical Research: Atmospheres*, *125*(5), e2019JD031480. https://doi.org/10.1029/2019jd031480

Malm, W., & Hand, J. L. (2007). An examination of the physical and optical properties of aerosols collected in the IMPROVE program. *Atmospheric Environment*, *41*(16), 3407–3427. https://doi.org/10.1016/j.atmosenv.2006.12.012

Malm, W. C., Pitchford, M. L., McDade, C., & Ashbaugh, L. L. (2007). Coarse particle speciation at selected locations in the rural continental United States. *Atmospheric Environment*, *41*(10), 2225–2239. https://doi.org/10.1016/j.atmosenv.2006.10.077

Malm, W. C., Schichtel, B. A., Ames, R. B., & Gebhart, K. A. (2002). A 10-year spatial and temporal trend of sulfate across the United States. *Journal of Geophysical Research*, *107*(D22), 4627. https://doi.org/10.1029/2002JD002107

Malm, W. C., Schichtel, B. A., Hand, J. L., & Collett Jr, J. L. (2017). Concurrent temporal and spatial trends in sulfate and organic mass concentrations measured in the IMPROVE monitoring program. *Journal of Geophysical Research: Atmospheres*, *122*(19), 10462–10476. https://doi.org/10.1002/2017JD026865

Malm, W. C., Schichtel, B. A., & Pitchford, M. L. (2011). Uncertainties in PM2. 5 gravimetric and speciation measurements and what we can learn from them. *Journal of the Air and Waste Management Association*, *61*(11), 1131–1149. https://doi.org/10.1080/10473289.2011.603998

Malm, W. C., Schichtel, B. A., Pitchford, M. L., Ashbaugh, L. L., & Eldred, R. A. (2004). Spatial and monthly trends in speciated fine particle concentration in the United States. *Journal of Geophysical Research*, *109*(D3). https://doi.org/10.1029/2003JD003739

Malm, W. C., Sisler, J. F., Huffman, D., Eldred, R. A., & Cahill, T. A. (1994). Spatial and seasonal trends in particle concentration and optical extinction in the United States. *Journal of Geophysical Research*, *99*(D1), 1347–1370. https://doi.org/10.1029/93JD02916

McNamara, S. M., Kolesar, K. R., Wang, S., Kirpes, R. M., May, N. W., Gunsch, M. J., et al. (2020). Observation of road salt aerosol driving inland wintertime atmospheric chlorine chemistry. *ACS Central Science*, *6*(5), 684–694. https://doi.org/10.1021/acscentsci.9b00994

Murphy, D. M., Chow, J. C., Leibensperger, E. M., Malm, W. C., Pitchford, M., Schichtel, B. A., et al. (2011). Decreases in elemental carbon and fine particle mass in the United States. *Atmospheric Chemistry and Physics*, *11*(10), 4679–4686. https://doi.org/10.5194/acp-11-4679-2011

Murphy, D. M., Froyd, K. D., Bian, H., Brock, C. A., Dibb, J. E., DiGangi, J. P., et al. (2019). The distribution of sea-salt aerosol in the global troposphere. *Atmospheric Chemistry and Physics*, *19*(6), 4093–4104. https://doi.org/10.5194/acp-19-4093-2019

Newberg, J. T., Matthew, B. M., & Anastasio, C. (2005). Chloride and bromide depletions in sea-salt particles over the northeastern Pacific Ocean. *Journal of Geophysical Research*, *110*(D6). https://doi.org/10.1029/2004JD005446

Nopmongcol, U., Beardsley, R., Kumar, N., Knipping, E., & Yarwood, G. (2019). Changes in United States deposition of nitrogen and sulfur compounds over five decades from 1970 to 2020. *Atmospheric Environment*, *209*, 144–151. https://doi.org/10.1016/j.atmosenv.2019.04.018

Perry, K. D., Cahill, T. A., Eldred, R. A., Dutcher, D. D., & Gill, T. E. (1997). Long-range transport of North African dust to the eastern United States. *Journal of Geophysical Research*, *102*(D10), 11225–11238. https://doi.org/10.1029/97JD00260

Petzold, A., Ogren, J. A., Fiebig, M., Laj, P., Li, S. M., Baltensperger, U., et al. (2013). Recommendations for reporting "black carbon" measurements. *Atmospheric Chemistry and Physics*, *13*(16), 8365–8379. https://doi.org/10.5194/acp-13-8365-2013

Philip, S., Martin, R., Pierce, J., Jimenez, J.-L., Zhang, Q., Canagaratna, M., et al. (2014). Spatially and seasonally resolved estimate of the ratio of organic mass to organic carbon. *Atmospheric Environment*, *87*, 34–40. https://doi.org/10.1016/j.atmosenv.2013.11.065

Pi, H., Sharratt, B., Schillinger, W. F., Bary, A., & Cogger, C. (2018). Chemical composition of windblown dust emitted from agricultural soils amended with biosolids. *Aeolian Research*, *32*, 102–115. https://doi.org/10.1016/j.aeolia.2018.02.001

Pitchford, M., Poirot, R., Schichtel, B. A., & Malm, W. C. (2009). Characterization of the winter midwestern particulate nitrate bulge. *Journal of the Air and Waste Management Association*, *59*(9), 1061–1069. https://doi.org/10.3155/1047-3289.59.9.1061

Polidori, A., Turpin, B. J., Davidson, C. I., Rodenburg, L. A., & Maimone, F. (2008). Organic PM 2.5: Fractionation by polarity, FTIR spectroscopy, and OM/OC ratio for the Pittsburgh aerosol. *Aerosol Science and Technology*, *42*(3), 233–246. https://doi.org/10.1080/02786820801958767

Pope, R., Stanley, K. M., Domsky, I., Yip, F., Nohre, L., & Mirabelli, M. C. (2017). The relationship of high PM2. 5 days and subsequent asthma-related hospital encounters during the fireplace season in Phoenix, AZ, 2008–2012. *Air Quality, Atmosphere & Health*, *10*(2), 161–169. https://doi.org/10.1007/s11869-016-0431-2

Prein, A. F., Coen, J., & Jaye, A. (2022). The character and changing frequency of extreme California fire weather. *Journal of Geophysical Research: Atmospheres*, *127*(9), e2021JD035350. https://doi.org/10.1029/2021JD035350

Prenni, A., Day, D., Evanoski-Cole, A., Sive, B., Hecobian, A., Zhou, Y., et al. (2016). Oil and gas impacts on air quality in federal lands in the Bakken region: An overview of the Bakken air quality study and first results. *Atmospheric Chemistry and Physics*, *16*(3), 1401–1416. https://doi.org/10.5194/acp-16-1401-2016

Prenni, A., Hand, J., Malm, W., Copeland, S., Luo, G., Yu, F., et al. (2019). An examination of the algorithm for estimating light extinction from IMPROVE particle speciation data. *Atmospheric Environment*, *214*, 116880. https://doi.org/10.1016/j.atmosenv.2019.116880

Prospero, J. M., Delany, A. C., Delany, A. C., & Carlson, T. N. (2021). The discovery of African dust transport to the western Hemisphere and the Saharan air layer: A history. *Bulletin of the American Meteorological Society*, *102*(6), E1239–E1260. https://doi.org/10.1175/BAMS-D-19-0309.1

Prospero, J. M., Ginoux, P., Torres, O., Nicholson, S. E., & Gill, T. E. (2002). Environmental characterization of global sources of atmospheric soil dust identified with the Nimbus 7 Total Ozone Mapping Spectrometer (TOMS) absorbing aerosol product. *Reviews of Geophysics*, *40*(1), 1002. https://doi.org/10.1029/2000RG000095

Pu, B., & Ginoux, P. (2018). Climatic factors contributing to long-term variations in surface fine dust concentration in the United States. *Atmospheric Chemistry and Physics*, *18*(6), 4201–4215. https://doi.org/10.5194/acp-18-4201-2018

Rivera, N. I. R., Gill, T. E., Gebhart, K. A., Hand, J. L., Bleiweiss, M. P., & Fitzgerald, R. M. (2009). Wind modeling of Chihuahuan Desert dust outbreaks. *Atmospheric Environment*, *43*(2), 347–354. https://doi.org/10.1016/j.atmosenv.2008.09.069

Robinson, E. S., Battaglia, M., Jr., Campbell, J. R., Cesler-Maloney, M., Simpson, W., Mao, J. Q., et al. (2024). Multi-year, high-time resolution aerosol chemical composition and mass measurements from Fairbanks, Alaska. *Environmental Science-Atmospheres*, *4*(6), 685–698. https://doi.org/10.1039/d4ea00008k

Rogge, W. F., Medeiros, P. M., & Simoneit, B. R. (2007). Organic marker compounds in surface soils of crop fields from the San Joaquin Valley fugitive dust characterization study. *Atmospheric Environment*, *41*(37), 8183–8204. https://doi.org/10.1016/j.atmosenv.2007.06.030

Russell, A., Valin, L., & Cohen, R. (2012). Trends in OMI NO2 observations over the United States: Effects of emission control technology and the economic recession. *Atmospheric Chemistry and Physics*, *12*(24), 12197–12209. https://doi.org/10.5194/acp-12-12197-2012

Ruthenburg, T. C., Perlin, P. C., Liu, V., McDade, C. E., & Dillner, A. M. (2014). Determination of organic matter and organic matter to organic carbon ratios by infrared spectroscopy with application to selected sites in the IMPROVE network. *Atmospheric Environment*, *86*, 47–57. https://doi.org/10.1016/j.atmosenv.2013.12.034

Safford, H. D., Paulson, A. K., Steel, Z. L., Young, D. J. N., & Wayman, R. B. (2022). The 2020 California fire season: A year like no other, a return to the past or a harbinger of the future? *Global Ecology and Biogeography*, *31*(10), 2005–2025. https://doi.org/10.1111/geb.13498

Schichtel, B. A., Hand, J. L., Barna, M. G., Gebhart, K. A., Copeland, S., Vimont, J., & Malm, W. C. (2017). Origin of fine particulate carbon in the rural United States. *Environmental Science and Technology*, *51*(17), 9846–9855. https://doi.org/10.1021/acs.est.7b00645

Shah, V., Jaeglé, L., Thornton, J. A., Lopez-Hilfiker, F. D., Lee, B. H., Schroder, J. C., et al. (2018). Chemical feedbacks weaken the wintertime response of particulate sulfate and nitrate to emissions reductions over the eastern United States. *Proceedings of the National Academy of Sciences of the United States of America*, *115*(32), 8110–8115. https://doi.org/10.1073/pnas.1803295115

Shi, L., Zhu, Q., Wang, Y., Liu, P., Zhang, H., Schwartz, J., et al. (2022). Incident dementia and long-term exposure to constituents of fine particle air pollution: A national cohort study in the United States. *Proceedings of the National Academy of Sciences of the United States of America*, *120*(1). https://doi.org/10.1073/pnas.2211282119

Sickles, J. E., & Shadwick, D. S. (2015). Air quality and atmospheric deposition in the eastern US: 20 years of change. *Atmospheric Chemistry and Physics*, *15*(1), 173–197. https://doi.org/10.5194/acp-15-173-2015

Silvern, R. F., Jacob, D. J., Kim, P. S., Marais, E. A., Turner, J. R., Campuzano-Jost, P., & Jimenez, J. L. (2017). Inconsistency of ammonium–sulfate aerosol ratios with thermodynamic models in the eastern US: A possible role of organic aerosol. *Atmospheric Chemistry and Physics*, *17*(8), 5107–5118. https://doi.org/10.5194/acp-17-5107-2017

Simon, H., Bhave, P., Swall, J., Frank, N., & Malm, W. (2011). Determining the spatial and seasonal variability in OM/OC ratios across the US using multiple regression. *Atmospheric Chemistry and Physics*, *11*(6), 2933–2949. https://doi.org/10.5194/acp-11-2933-2011

Solomon, P. A., Crumpler, D., Flanagan, J. B., Jayanty, R. K. M., Rickman, E. E., & McDade, C. E. (2014). U.S. National PM2.5 chemical speciation monitoring networks—CSN and IMPROVE: Description of networks. *Journal of the Air and Waste Management Association*, *64*(12), 1410–1438. https://doi.org/10.1080/10962247.2014.956904

Spada, N. J., & Hyslop, N. P. (2018). Comparison of elemental and organic carbon measurements between IMPROVE and CSN before and after method transitions. *Atmospheric Environment*, *178*, 173–180. https://doi.org/10.1016/j.atmosenv.2018.01.043

Tong, D., Dan, M., Wang, T., & Lee, P. (2012). Long-term dust climatology in the western United States reconstructed from routine aerosol ground monitoring. *Atmospheric Chemistry and Physics*, *12*(11), 5189–5205. https://doi.org/10.5194/acp-12-5189-2012

Tong, D. Q., Gill, T. E., Sprigg, W. A., Van Pelt, R. S., Baklanov, A. A., Barker, B. M., et al. (2023). Health and safety effects of airborne soil dust in the Americas and beyond. *Reviews of Geophysics*, *61*(2), e2021RG000763. https://doi.org/10.1029/2021RG000763

Tong, D. Q., Lamsal, L., Pan, L., Ding, C., Kim, H., Lee, P., et al. (2015). Long-term NOx trends over large cities in the United States during the great recession: Comparison of satellite retrievals, ground observations, and emission inventories. *Atmospheric Environment*, *107*, 70–84. https://doi.org/10.1016/j.atmosenv.2015.01.035

Turpin, B. J., Saxena, P., & Andrews, E. (2000). Measuring and simulating particulate organics in the atmosphere: Problems and prospects. *Atmospheric Environment*, *34*(18), 2983–3013. https://doi.org/10.1016/S1352-2310(99)00501-4

Vitousek, P. M., Aber, J. D., Howarth, R. W., Likens, G. E., Matson, P. A., Schindler, D. W., et al. (1997). Human alteration of the global nitrogen cycle: Sources and consequences. *Ecological Applications*, *7*(3), 737–750. https://doi.org/10.1890/1051-0761(1997)007[0737:HAOTGN]2.0.CO;2

Warner, J., Dickerson, R., Wei, Z., Strow, L., Wang, Y., & Liang, Q. (2017). Increased atmospheric ammonia over the world's major agricultural areas detected from space. *Geophysical Research Letters*, *44*(6), 2875–2884. https://doi.org/10.1002/2016GL072305

Weber, R. J., Guo, H., Russell, A. G., & Nenes, A. (2016). High aerosol acidity despite declining atmospheric sulfate concentrations over the past 15 years. *Nature Geoscience*, *9*(4), 282–285. https://doi.org/10.1038/NGEO2665

Wei, J., Wang, J., Li, Z., Kondragunta, S., Anenberg, S., Wang, Y., et al. (2023). Long-term mortality burden trends attributed to black carbon and PM2.5 from wildfire emissions across the continental USA from 2000 to 2020: A deep learning modelling study. *Lancet*, *7*(7), e963–e975. https://doi.org/10.1016/S2542-5196(23)00235-8

White, W. H. (2008). Chemical markers for sea salt in IMPROVE aerosol data. *Atmospheric Environment*, *42*(2), 261–274. https://doi.org/10.1016/j.atmosenv.2007.09.040

Wilmot, T., Hallar, A., Lin, J., & Mallia, D. (2021). Expanding number of Western US urban centers face declining summertime air quality due to enhanced wildland fire activity. *Environmental Research Letters*, *16*(5), 054036. https://doi.org/10.1088/1748-9326/abf966

Xue, Z., Gupta, P., & Christopher, S. (2021). Satellite-based estimation of the impacts of summertime wildfires on PM 2.5 concentration in the United States. *Atmospheric Chemistry and Physics*, *21*(14), 11243–11256. https://doi.org/10.5194/acp-21-11243-2021

Young, D. E. (2015). Analysis lab contract transition. In *CSN data Advisory*. Retrieved from https://airquality.ucdavis.edu/sites/g/files/dgvnsk1671/files/inline-files/CSN_contract_transition_data_advisory_final_508.pdf

Yu, H., Tan, Q., Zhou, L., Zhou, Y., Bian, H., Chin, M., et al. (2021). Observation and modeling of the historic "Godzilla" African dust intrusion into the Caribbean basin and the southern US in June 2020. *Atmospheric Chemistry and Physics*, *21*(16), 12359–12383. https://doi.org/10.5194/acp-21-12359-2021

Yu, K. A., McDonald, B. C., & Harley, R. A. (2021). Evaluation of nitrogen oxide emission inventories and trends for on-road gasoline and diesel vehicles. *Environmental Science and Technology*, *55*(10), 6655–6664. https://doi.org/10.1021/acs.est.1c00586

Zhang, X., Trzepla, K., White, W., & Hyslop, N. P. (2022). Quantifying residual elemental carbon by thermal-optical analysis using an extended IMPROVE_A protocol with higher maximum temperature. *Journal of the Air and Waste Management Association*, *72*(11), 1316–1325. https://doi.org/10.1080/10962247.2022.2119306

Zhang, Y., Mathur, R., Bash, J. O., Hogrefe, C., Xing, J., & Roselle, S. J. (2018). Long-term trends in total inorganic nitrogen and sulfur deposition in the US from 1990 to 2010. *Atmospheric Chemistry and Physics*, *18*(12), 9091–9106. https://doi.org/10.5194/acp-18-9091-2018